

ENERGY FLOW MODELLING OF INTERCONNECTED STRUCTURES: A DETERMINISTIC FOUNDATION FOR STATISTICAL ENERGY ANALYSIS

YASUO KISHIMOTO

Kougi-Tai Hijitsu-Gun, Gifu Air Base, Mubanchi Naka Kanyuchi, 504 Japan

DENNIS S. BERNSTEIN

*Department of Aerospace Engineering, University of Michigan, Ann Arbor, Michigan
48109-2118, U.S.A.*

AND

STEVEN R. HALL

*Department of Aeronautics and Astronautics, Massachusetts Institute of Technology,
Cambridge, MA 02139, U.S.A.*

(Received 1 September 1993, and in final form 8 September 1994)

Energy flow models are derived for interconnected structures in terms of both modal and structural subsystems. The principal goal of this analysis is to develop a deterministic foundation for energy flow analysis that clarifies assumptions under which statistical energy analysis (SEA) predictions are valid. Three sources of error involving modal incoherence, pairwise coupling loss factor and blocked modal energy are identified. Assumptions under which these terms are negligible are identified and compared to standard SEA assumptions.

© 1995 Academic Press Limited

1. INTRODUCTION

The analysis of complicated structures comprised of multiple substructures remains one of the most challenging problems in structural dynamics. As with the analysis of complex systems in general, it is highly desirable to analyze the overall system in terms of the interaction of system components. The underlying idea is to use insight into the interaction of a small number of subsystems to predict the behavior of a large-scale system with numerous interacting components. In the area of structural dynamics, energy flow methods such as statistical energy analysis (SEA) [1–26] seek to predict vibration levels of complicated structures in terms of the energy flow interaction of pairs of modes. For high-dimensional problems with significant uncertainty, these methods complement finite element modelling techniques.

As may be expected, the ability to predict the behavior of a complicated system in terms of the pairwise interaction of subsystems is limited by the extent to which the interaction of a pair of subsystems is affected by the presence of additional subsystems. Fortunately, in many large-scale structural vibration problems, such extraneous interactions are small due to weak coupling and other effects. It is these effects that SEA exploits to facilitate the analysis of complex structures.

The early work on SEA is based on the classical papers [1–7] as well as many others. In more recent work researchers have calculated energy flow between two interconnected structures using deterministic methods. In particular, Pan *ET AL.* [24] calculated the energy flow between a rigid body and supporting panel by using a modal approach, Mace [22] calculated the energy flow between two interconnected beams by using wave functions, and Keane and Price [15,20] obtained SEA-type relations for a pair of interconnected structures. However, the deterministic energy flow models derived in references [22,24] are different from the fundamental equations used in SEA which characterize energy flow in terms of energy differences.

For multiple interconnected substructures there have been several attempts to reconcile the differences between deterministic approaches and SEA [9,11,13,14,17]. For example, Maidanik [9] developed a theoretical foundation for SEA by using an energy flow model, Hodges and Woodhouse [14] explained SEA properties from a physical point of view, and Langley [17] provided a general development of SEA relations. Nevertheless, there does not yet exist a complete theory of SEA that rigorously clarifies the assumptions that underlie the methodology. The goal of this paper is thus to make progress in clarifying the precise assumptions under which SEA predictions are valid.

To this end, we extend our previous work [27], which was motivated by reference [28], to obtain energy flow models for interconnected structures. In particular, we derive two distinct energy flow models, namely, the modal subsystem model (section 3), which views each mode as a subsystem, and the structural subsystem model (section 4), which views each structure as a subsystem. These energy flow models predict energy flow among modes or structures independently of the number of interconnected structures and the coupling strength. These results are based on the thermodynamic energy flow relationship given by Theorem 3.2 of reference [27], which is analogous to the corresponding result given by equation (37) of reference [17] involving subsystem kinetic energy.

Crucial features of our development include the exclusive use of a deterministic structural model and a localized stochastic disturbance. This formulation stands in contrast to treatments that invoke stochastic structural uncertainty models and spatially distributed disturbances to justify energy flow relationships [8,29–31]. We believe that energy flow predictions based on deterministic modelling leave less ambiguity with regard to the meaning of the results than predictions based on stochastic modelling that invoke the notion of an ensemble or statistical population of structures. For this reason our derivation of SEA results intentionally seeks to de-emphasize the statistical aspect of the theory.

In developing a rigorous foundation for SEA-type predictions, we consider three sources of error, namely, modal incoherence, the pairwise coupling coefficient, and the use of blocked modal energy. SEA often invokes a modal incoherence assumption so that energy flow among structures can be represented by a modal flow model. Modal incoherence, however, occurs when the disturbances are spatially distributed “rain on the roof” [9,14,26] or when the covariance is averaged over an uncertainty distribution [32]. Our analysis shows that modal incoherence is responsible for discrepancies between energy flow predictions based on the modal subsystem model and energy flow predictions based on the structural subsystem model. Furthermore, in SEA the coupling coefficient is derived from the pairwise interaction of modes in isolation from other modes. As in reference [27], however, the coupling coefficients are influenced by the presence of other modes. In our development, the coupling coefficients are decomposed into pairwise interaction terms as well as error terms. Finally, as shown in reference [27], energy actually flows according to *thermodynamic energy* and not according to blocked energy. Although thermodynamic energy coincides with uncoupled energy for second order subsystems, there is a significant difference between thermodynamic energy and blocked energy. Consequently, SEA inevitably incurs errors due

to all these effects. In this paper we quantify these error terms and consider limiting conditions under which these error terms vanish. For cases in which the error terms are small, the results thus predict that energy flow is proportional to blocked energy, as in classical SEA theory. A numerical example involving a pair of cantilevered beams is used to illustrate these results.

2. STRUCTURAL MODEL

We consider r one- or two-dimensional structures under vibration by means of pointwise external disturbance forces. Each pair of structures is assumed to be mutually interconnected by means of conservative couplings. For convenience, we make the simplifying assumption that all couplings to a given structure are connected to a single point on that structure. The case of structures interconnected at multiple points is more complicated and is outside the scope of this paper.

The partial differential equation for the displacement response $\chi_i(\xi, t)$ of the i th structure is given by

$$\rho_i(\xi) \frac{\partial^2 \chi_i(\xi, t)}{\partial t^2} + \mathcal{L}_i \chi_i(\xi, t) = \tilde{w}_i(t) \delta(\xi - \xi_i) - h_i(\xi, \xi_{c_i}, t), \quad (1)$$

where $\xi \in \Omega_i$ denotes the spatial co-ordinate defined on a region Ω_i for the i th structure. Furthermore, $\rho_i(\xi)$ is the mass density of the i th structure, \mathcal{L}_i is the self-adjoint stiffness operator for the i th structure, and $\tilde{w}_i(t)$ is the external disturbance force acting on the i th structure at the point ξ_i . We assume that $\tilde{w}_i(t)$, $i = 1, \dots, r$, are mutually uncorrelated white noise disturbances with unit intensity. Additionally, the coupling effect $h_i(\xi, \xi_{c_i}, t)$ at the coupling position ξ_{c_i} is given by

$$h_i(\xi, \xi_{c_i}, t) \triangleq f_i(t) \delta(\xi - \xi_{c_i}), \quad (2)$$

for an interaction force $f_i(t)$ and

$$h_i(\xi, \xi_{c_i}, t) \triangleq g_i(t) \delta'(\xi - \xi_{c_i}), \quad (3)$$

for an interaction torque $g_i(t)$, where $\delta'(x)$ is the doublet (derivative of the delta function).

We consider a modal decomposition of the i th structure of the form

$$\chi_i(\xi, t) = \sum_{j=1}^{\infty} q_{ij}(t) \psi_{ij}(\xi), \quad i = 1, \dots, r, \quad (4)$$

where $q_{ij}(t)$ and $\psi_{ij}(\xi)$ denote the modal co-ordinates and normalized eigenfunctions, respectively, and the double subscript ij denotes the j th mode of the i th structure. The normalized eigenfunctions $\psi_{ij}(\xi)$ satisfy the orthogonality properties

$$\int_{\Omega_i} \rho_i(\xi) \psi_{ij}(\xi) \psi_{ik}(\xi) d\xi = \delta_{jk}, \quad \int_{\Omega_i} \mathcal{L}_i \psi_{ij}(\xi) \psi_{ik}(\xi) d\xi = \omega_{ij}^2 \delta_{jk}, \quad (5)$$

where ω_{ij} is the uncoupled natural frequency of the j th mode of the i th structure and δ_{jk} is the Kronecker delta. From equations (4), (5) and appropriate boundary conditions, it follows that the modal co-ordinates $q_{ij}(t)$ satisfy

$$\ddot{q}_{ij}(t) + 2\zeta_{ij} \omega_{ij} \dot{q}_{ij}(t) + \omega_{ij}^2 q_{ij}(t) = a_{ij} \tilde{w}_i(t) - b_{ij} v_i(t), \quad (6)$$

where $v_i(t)$ is the coupling interaction and the modal damping term $2\zeta_{ij}\omega_{ij}\dot{q}_{ij}(t)$ is now included. In equation (6), the modal coefficient a_{ij} is defined by

$$a_{ij} \triangleq \psi_{ij}(\xi_i), \quad (7)$$

while

$$b_{ij} \triangleq \psi_{ij}(\xi_{ci}), \quad v_i(t) \triangleq f_i(t), \quad (8)$$

for force interaction and

$$b_{ij} \triangleq \frac{\partial \psi_{ij}(\xi_{ci})}{\partial \xi}, \quad v_i(t) \triangleq g_i(t), \quad (9)$$

for torque interaction.

The modal velocity $y_{ij}(t)$ of the j th mode of the i th structure and the velocity $y_i(t)$ of the i th structure at the coupling point are given by

$$y_{ij}(t) = b_{ij}\dot{q}_{ij}(t), \quad y_i(t) = \sum_{j=1}^{n_i} y_{ij}(t), \quad (10,11)$$

where n_i is the number of modes of the i th structure in the frequency range of interest.

Henceforth we consider stiffness coupling in which case the coupling interaction $v_i(t)$ is given by

$$v_i(t) = \sum_{\substack{p=1 \\ p \neq i}}^r K_{ip} \left[\sum_{j=1}^{n_i} b_{ij}q_{ij}(t) - \sum_{q=1}^{n_p} b_{pq}q_{pq}(t) \right], \quad (12)$$

where K_{ip} is the stiffness of the coupling between the i th and the p th structures. The results of this paper can be extended to the case of dissipative coupling by applying the results of reference [33].

For later use, note that the modal impedance $z_{ij}(s)$, $i = 1, \dots, r$, $j = 1, \dots, n_i$, is given by

$$z_{ij}(s) = (s^2 + 2\zeta_{ij}\omega_{ij}s + \omega_{ij}^2)/s. \quad (13)$$

In the following two sections we derive two distinct energy flow models based upon equation (6).

3. ENERGY FLOW MODELLING: MODAL SUBSYSTEMS

First, we obtain the modal subsystem model by treating each mode as a subsystem. Let $w_{ij}(t)$ denote the disturbance force exciting the j th mode of the i th structure, that is,

$$w_{ij}(t) \triangleq a_{ij}\tilde{w}_i(t), \quad i = 1, \dots, r, j = 1, \dots, n_i, \quad (14)$$

and let $L(s)$ denote the $r \times r$ stiffness coupling transfer function given by

$$L(s) = \frac{1}{s}C_L, \quad (15)$$

where

$$C_L \triangleq \begin{bmatrix} \sum_{p=2}^r K_{1p} & -K_{12} & \dots & -K_{1r} \\ -K_{12} & \sum_{\substack{p=1 \\ p \neq 2}}^r K_{2p} & \dots & -K_{2r} \\ \vdots & \vdots & \vdots & \vdots \\ -K_{1r} & -K_{2r} & \dots & \sum_{p=1}^{r-1} K_{pr} \end{bmatrix}, \quad (16)$$

so that from equations (10)–(12) the coupling interaction $v_i(t)$ and the structural velocity $y_i(t)$ are related by

$$v_s = L(s)y_s, \quad (17)$$

where $y_s(t) \triangleq [y_1(t) \cdots y_r(t)]^T$ and $v_s(t) \triangleq [v_1(t) \cdots v_r(t)]^T$.

To obtain a feedback representation of the interconnected modal subsystems, we define the modal impedance matrix

$$Z_m(s) \triangleq \text{diag}(z_{11}(s), \dots, z_{1n_1}(s), \dots, z_{r1}(s), \dots, z_{rn_r}(s)), \quad (18)$$

and the vectors

$$y_m(t) \triangleq [\dot{q}_{11}(t) \cdots \dot{q}_{1n_1}(t) \cdots \dot{q}_{r1}(t) \cdots \dot{q}_{rn_r}(t)]^T, \quad (19)$$

$$w_m(t) \triangleq [w_{11}(t) \cdots w_{1n_1}(t) \cdots w_{r1}(t) \cdots w_{rn_r}(t)]^T, \quad (20)$$

$$v_m(t) \triangleq [b_{11}v_1(t) \cdots b_{1n_1}v_1(t) \cdots b_{r1}v_r(t) \cdots b_{rn_r}v_r(t)]^T, \quad (21)$$

$$\tilde{w}(t) \triangleq [\tilde{w}_1(t) \cdots \tilde{w}_r(t)]^T. \quad (22)$$

Note that $w_m(t) = D_m \tilde{w}(t)$, $y_s(t) = E_m^T y_m(t)$ and $v_m(t) = E_m v_s(t)$, where the matrices D_m and E_m are defined by

$$D_m \triangleq \begin{bmatrix} a_{11} & \cdots & a_{1n_1} & 0 & \cdots & 0 & 0 & \cdots & 0 & 0 & \cdots & 0 \\ 0 & \cdots & 0 & a_{21} & \cdots & a_{2n_2} & 0 & \cdots & 0 & 0 & \cdots & 0 \\ \vdots & \vdots & \vdots & \vdots & \vdots & \vdots & \vdots & \vdots & \vdots & \vdots & \vdots & \vdots \\ 0 & \cdots & 0 & 0 & \cdots & 0 & 0 & \cdots & 0 & a_{r1} & \cdots & a_{rn_r} \end{bmatrix}^T, \quad (23)$$

$$E_m \triangleq \begin{bmatrix} b_{11} & \cdots & b_{1n_1} & 0 & \cdots & 0 & 0 & \cdots & 0 & 0 & \cdots & 0 \\ 0 & \cdots & 0 & b_{21} & \cdots & b_{2n_2} & 0 & \cdots & 0 & 0 & \cdots & 0 \\ \vdots & \vdots & \vdots & \vdots & \vdots & \vdots & \vdots & \vdots & \vdots & \vdots & \vdots & \vdots \\ 0 & \cdots & 0 & 0 & \cdots & 0 & 0 & \cdots & 0 & b_{r1} & \cdots & b_{rn_r} \end{bmatrix}^T. \quad (24)$$

With this notation, the interconnected system (6) can be expressed as the feedback system shown in Figure 1, where $u_m(t) \triangleq w_m(t) - v_m(t)$ and the coupling matrix $L_m(s)$ for the modal subsystem energy flow model satisfying $v_m = L_m y_m$ is defined by

$$L_m(s) \triangleq E_m L(s) E_m^T. \quad (25)$$

Note that since $L(s)$ given by equation (15) is conservative, that is, $L(j\omega) + L^*(j\omega) = 0$, it follows that

$$\begin{aligned} L_m(j\omega) + L_m^*(j\omega) &= E_m L(j\omega) E_m^T + (E_m L(j\omega) E_m^T)^* \\ &= E_m (L(j\omega) + L^*(j\omega)) E_m^T \\ &= 0, \end{aligned} \quad (26)$$

so that $L_m(s)$ is also conservative. Since the modal impedance matrix $Z_m(s)$ is strictly positive real and the coupling $L_m(s)$ is conservative, it follows from standard results that the closed-loop system in Figure 1 is asymptotically stable [27].

As in reference [27], the steady-state average modal energy flows per unit bandwidth $E_{ij}^c(\omega)$, $E_{ij}^d(\omega)$, $E_{ij}^e(\omega)$, $i = 1, \dots, r$, $j = 1, \dots, n_i$ are defined by

$$\begin{aligned} E_{ij}^c(\omega) &\triangleq -\frac{1}{2} \operatorname{Re} S_{v_m v_m}(\omega)_{ijij}, & E_{ij}^d(\omega) &\triangleq -\frac{1}{2} \operatorname{Re} S_{u_m v_m}(\omega)_{ijij}, \\ E_{ij}^e(\omega) &\triangleq \frac{1}{2} \operatorname{Re} [S_{w_m v_m}(\omega)_{ijij}], \end{aligned} \quad (27)$$

where $S_{v_m v_m}$, $S_{u_m v_m}$, and $S_{w_m v_m}$ denote the cross-spectral densities of the given signals, $E_{ij}^c(\omega)$ is the energy flow entering the j th mode of i th structure through the coupling $L_m(s)$, $E_{ij}^d(\omega)$ is the energy dissipation rate of the j th mode of the i th structure, and $E_{ij}^e(\omega)$ is the external energy flow entering the j th mode of the i th structure. In equation (27) and throughout the paper, the shorthand A_{ijpq} is used to denote the element $A_{(n_{ij}, n_{pq})}$ of an arbitrary matrix A , where n_{ij} is the mode count index defined by

$$n_{ij} \triangleq \left(\sum_{l=1}^{i-1} n_l \right) + j. \quad (28)$$

The following result is obtained from reference [27].

Proposition 3.1. For $i = 1, \dots, r$ and $j = 1, \dots, n_i$, the modal coupling, dissipative, and external energy flows per unit bandwidth $E_{ij}^c(\omega)$, $E_{ij}^d(\omega)$ and $E_{ij}^e(\omega)$ are given by

$$E_{ij}^c(\omega) = -\frac{1}{2\pi} \operatorname{Re} [L(j\omega) (L_m(j\omega) + Z_m(j\omega))^{-1} S_{w_m v_m} (L_m(j\omega) + Z_m(j\omega))^{-*}]_{ijij}, \quad (29)$$

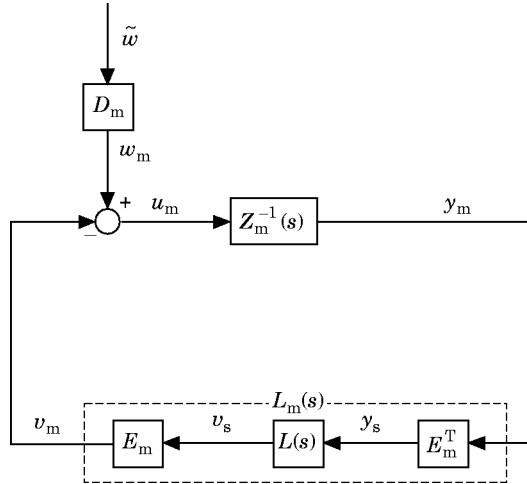


Figure 1. Feedback representation of modal subsystems.

$$E_{ij}^d(\omega) = -\frac{1}{2\pi} \operatorname{Re}[Z_m(j\omega)(L_m(j\omega) + Z_m(j\omega))^{-1} S_{w_m w_m} (L_m(j\omega) + Z_m(j\omega))^{-*}]_{ijj}, \quad (30)$$

$$E_{ij}^c(\omega) = \frac{1}{2\pi} \operatorname{Re}[S_{w_m w_m} (L_m(j\omega) + Z_m(j\omega))^{-*}]_{ijj}, \quad (31)$$

where $S_{w_m w_m}$ is the intensity matrix of $w_m(t)$ given by $S_{w_m w_m} = D_m D_m^T$.

To analyze energy flows among modal subsystems, we now define as in reference [27] the *cross-modal thermodynamic energy* E_{imn}^{th} of modes m and n of the i th structure and the *modal thermodynamic energy* E_{ij}^{th} of the j th mode of the i th structure for $i=1, \dots, r$ and $j, m, n=1, \dots, n_i$ as

$$E_{imn}^{\text{th}} \triangleq \frac{S_{w_m w_m m i n}}{2\sqrt{c_{im} c_{in}}} = \frac{a_{im} a_{in}}{2\sqrt{c_{im} c_{in}}}, \quad (32)$$

$$E_{ij}^{\text{th}} \triangleq E_{ijj}^{\text{th}} = \frac{S_{w_m w_m m i j}}{2c_{ij}} = \frac{a_{ij}^2}{2c_{ij}}, \quad (33)$$

respectively, where $c_{ij} \triangleq 2\zeta_{ij}\omega_{ij}$. Since $L_m(j\omega)$ has zero real part, the following results follow from Theorem 3.2 and Corollary 3.3 of reference [27].

Proposition 3.2. For $i=1, \dots, r$ and $j=1, \dots, n_i$, the modal coupling energy flow per unit bandwidth $E_{ij}^c(\omega)$ is given by

$$E_{ij}^c(\omega) = E_{\text{inc},ij}^c(\omega) + E_{\text{coh},ij}^c(\omega), \quad (34)$$

where

$$E_{\text{inc},ij}^c(\omega) \triangleq \sum_{k=1}^{n_i} \delta_{ijk}(\omega)(E_{ik}^{\text{th}} - E_{ij}^{\text{th}}) + \sum_{\substack{p=1 \\ p \neq i}}^r \sum_{q=1}^{n_p} \delta_{ijpq}(\omega)(E_{pq}^{\text{th}} - E_{ij}^{\text{th}}), \quad (35)$$

$$E_{\text{coh},ij}^c(\omega) \triangleq \sum_{k=1}^{n_i} \left[\sum_{\substack{l=1 \\ l \neq k}}^{n_i} \mu_{ijkl}(\omega) E_{ikl}^{\text{th}} - \sum_{\substack{l=1 \\ l \neq j}}^{n_i} \mu_{ikjl}(\omega) E_{ijl}^{\text{th}} \right], \quad (36)$$

and where $\delta_{ijpq}(\omega)$ and $\mu_{ijpq}(\omega)$ are defined by

$$\delta_{ijpq}(\omega) \triangleq \frac{1}{\pi} c_{ij} c_{pq} |[(Z_m(j\omega) + L_m(j\omega))^{-1}]_{ijpq}|^2, \quad (37)$$

$$\mu_{ijkl}(\omega) \triangleq \frac{c_{ij} \sqrt{c_{ik} c_{il}}}{\pi} \operatorname{Re}([(Z_m(j\omega) + L_m(j\omega))^{-1}]_{ijk} [(Z_m(j\omega) + L_m(j\omega))^{-*}]_{ilj}). \quad (38)$$

In equation (34), the first term $E_{\text{inc},ij}^c(\omega)$ depends on differences between thermodynamic modal energies generated from the incoherent (diagonal) portion $\text{Inc}[S_{w_m w_m}]$ of $S_{w_m w_m}$, while the second term $E_{\text{coh},ij}^c(\omega)$ arises from the cross-modal thermodynamic energies generated from the coherent (off-diagonal) portion $\text{Coh}[S_{w_m w_m}]$ of $S_{w_m w_m}$, that is, the effect of disturbance correlation on each mode.

We now consider the modal coupling, dissipative, and external energy flows defined by

$$\begin{aligned} P_{ij}^c &\triangleq \int_{-\infty}^{\infty} E_{ij}^c(\omega) d\omega, & P_{ij}^d &\triangleq \int_{-\infty}^{\infty} E_{ij}^d(\omega) d\omega, \\ P_{ij}^e &\triangleq \int_{-\infty}^{\infty} E_{ij}^e(\omega) d\omega. \end{aligned} \quad (39)$$

Let $Z_m^{-1}(s)$ have the realization

$$\dot{x}_m(t) = A_m x_m(t) + B_m u_m(t), \quad y_m(t) = C_{m1} x_m(t), \quad (40, 41)$$

and define the constant diagonal damping matrix

$$C_{md} \triangleq \text{diag}(c_{11}, \dots, c_{1n_1}, \dots, c_{r1}, \dots, c_{rn_r}). \quad (42)$$

Since $x_m(t)$ is comprised of the position vector $x_{pm}(t)$ and the velocity vector $y_m(t)$, we can introduce an output matrix C_{pm} so that $x_{pm}(t) = C_{pm} x_m(t)$. Then the feedback system in Figure 1 has the realization

$$\dot{x}_m(t) = \tilde{A}_m x_m(t) + \tilde{D}_m \tilde{w}(t), \quad v_m(t) = C_{m2} x_m(t), \quad (43, 44)$$

where $\tilde{A}_m \triangleq A_m - B_m E_m C_L E_m^T C_{pm}$, $\tilde{D}_m \triangleq B_m D_m$ and $C_{m2} \triangleq E_m C_L E_m^T C_{pm}$. With this notation the following result follows from Corollary 4.1 of reference [27].

Proposition 3.3. For $i = 1, \dots, r$ and $j = 1, \dots, n_i$, the modal energy flows P_{ij}^c , P_{ij}^d and P_{ij}^e are given by

$$P_{ij}^c = -(C_{m2} \tilde{Q}_m C_{m1}^T)_{ijj}, \quad P_{ij}^d = -(C_{md} C_{m1} \tilde{Q}_m C_{m1}^T)_{ijj}, \quad P_{ij}^e = \frac{1}{2} (D_m \tilde{D}_m^T C_{m1}^T)_{ijj}, \quad (45-47)$$

where the steady-state modal covariance $\tilde{Q}_m \triangleq \lim_{t \rightarrow \infty} \mathcal{E}[x_m(t) x_m^T(t)]$ satisfies the algebraic Lyapunov equation

$$0 = \tilde{A}_m \tilde{Q}_m + \tilde{Q}_m \tilde{A}_m^T + \tilde{D}_m \tilde{D}_m^T. \quad (48)$$

Furthermore, the following result is obtained from Lemma 3.1 and Corollaries 3.1 and 3.2 of reference [27].

Proposition 3.4. The modal energy flows per unit bandwidth $E_{ij}^c(\omega)$, $E_{ij}^d(\omega)$, $E_{ij}^e(\omega)$, and the modal energy flows P_{ij}^c , P_{ij}^d , P_{ij}^e satisfy

$$E_{ij}^c(\omega) + E_{ij}^d(\omega) + E_{ij}^e(\omega) = 0, \quad i = 1, \dots, r, \quad j = 1, \dots, n_i, \quad (49)$$

$$\sum_{i=1}^r \sum_{j=1}^{n_i} E_{ij}^c(\omega) = 0, \quad (50)$$

$$P_{ij}^c + P_{ij}^d + P_{ij}^e = 0, \quad i = 1, \dots, r, \quad j = 1, \dots, n_i, \quad (51)$$

and

$$\sum_{i=1}^r \sum_{j=1}^{n_i} P_{ij}^c = 0. \quad (52)$$

Equations (49) and (51) represent the energy balance at each modal subsystem, while equations (50) and (52) reflect the fact that the coupling is conservative. As an example, Figure 2 illustrates energy flow among four modes of two interconnected structures.

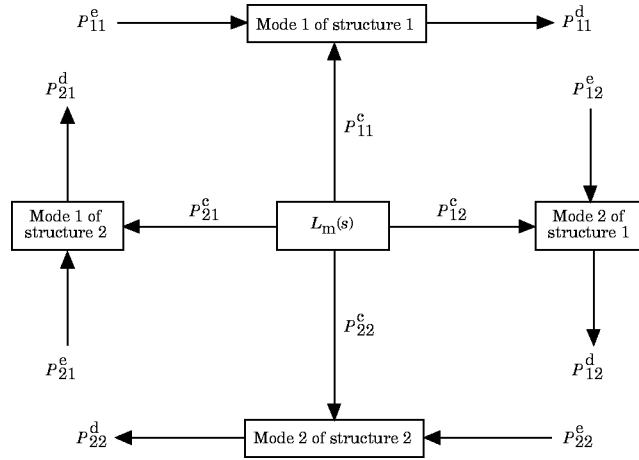


Figure 2. Energy flow model for two structures and four coupled modes.

4. ENERGY FLOW MODELLING: STRUCTURAL SUBSYSTEMS

We now obtain the structural subsystem energy flow model by treating each structure as a subsystem. In this model the energy flows are evaluated at the coupling points of the structures. Hence the colocated impedance $z_i(s)$ of the i th structure at the coupling point is given by

$$\frac{1}{z_i(s)} = \sum_{j=1}^{n_i} \frac{b_{ij}^2}{z_{ij}(s)}, \quad (53)$$

for $i=1, \dots, r$. Additionally, by using the fact that the admittance transfer function from the external force $\tilde{w}_i(t)$ applied at $\hat{\xi}_i$ to the velocity $y_i(t)$ at $\hat{\zeta}_i$ is given by $\sum_{j=1}^{n_i} a_{ij} b_{ij} / z_{ij}(s)$, (see p. 263 in reference [34]), it follows that the filter transfer function $T_i(s)$, defined by

$$T_i(s) \triangleq z_i(s) \sum_{j=1}^{n_i} \frac{a_{ij} b_{ij}}{z_{ij}(s)}, \quad (54)$$

transforms the external disturbance force \tilde{w}_i at $\hat{\xi}_i$ into the disturbance force w_i at the coupling point $\hat{\zeta}_i$, that is,

$$w_i = T_i \tilde{w}_i. \quad (55)$$

With the notation given in equations (54) and (55) and with $z_{ij}(s)$ given by equation (13), equation (6) can be rewritten as

$$z_i(s) y_i = w_i - v_i, \quad (56)$$

which corresponds to the electrical representation of the interconnected system shown in Figure 3 [27,28].

Since $z_i(s)$ is strictly positive real, it follows that

$$c_i(\omega) \triangleq \text{Re}[z_i(j\omega)] > 0, \quad i=1, \dots, r, \quad \omega \in \mathcal{R}, \quad (57)$$

where $c_i(\omega)$ is the frequency-dependent resistance or damping. For convenience, define the $r \times r$ diagonal transfer function

$$Z_s(s) \triangleq \text{diag}(z_1(s), \dots, z_r(s)), \quad (58)$$

and the frequency-dependent resistance or damping matrix

$$C_d(\omega) \triangleq \text{Re}[Z_s(j\omega)] = \text{diag}(c_1(\omega), \dots, c_r(\omega)). \quad (59)$$

With this notation, the interconnected system in equation (56) can be expressed as the feedback system in Figure 4, where $w_s(t) \triangleq [w_1(t) \cdots w_r(t)]^T$, $u_s(t) \triangleq [u_1(t) \cdots u_r(t)]^T = w_s(t) - v_s(t)$ and $y_s(t)$, $v_s(t)$ and $L(s)$ satisfy equation (17). Additionally, the components of $w_s(t)$ are mutually uncorrelated so that the power spectral density matrix $S_{w_s w_s}(\omega)$ of $w_s(t)$ has the form

$$S_{w_s w_s}(\omega) = \text{diag}(S_{w_1 w_1}(\omega), \dots, S_{w_r w_r}(\omega)), \quad (60)$$

where $S_{w_i w_i}(\omega)$ is the power spectral density of $w_i(t)$.

With this notation we can define structural energy flows per unit bandwidth $E_i^v(\omega)$, $E_i^d(\omega)$ and $E_i^y(\omega)$ for each structure. These flows correspond to $E_{ij}^v(\omega)$, $E_{ij}^d(\omega)$ and $E_{ij}^y(\omega)$ in the previous section where now $E_i^v(\omega)$ is the energy flow entering the i th structure through the

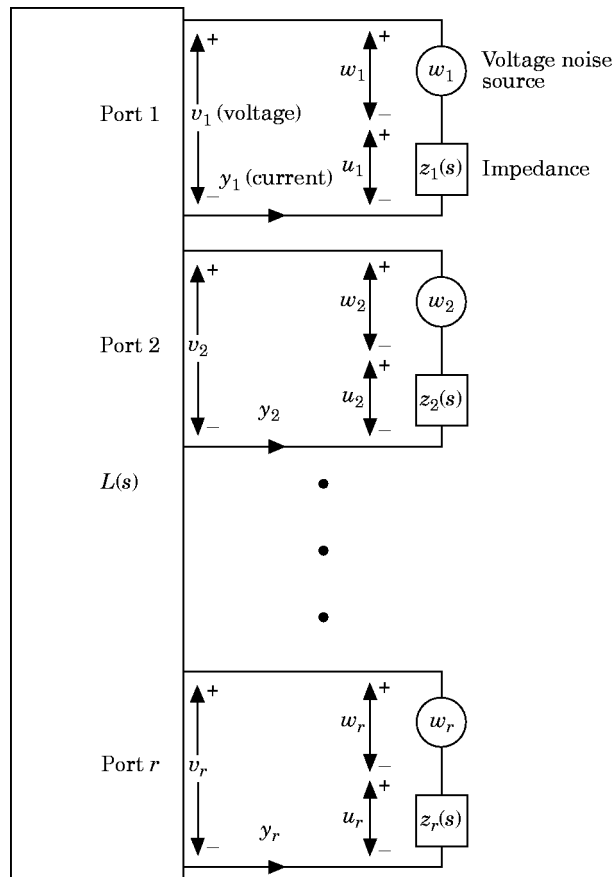


Figure 3. Electrical representation of structural subsystems.

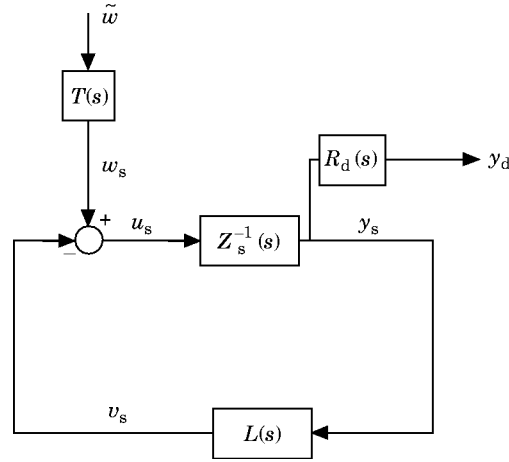


Figure 4. Feedback representation of structural subsystems.

coupling $L(s)$ in Figure 4. The following result corresponds to Proposition 3.1 in the previous section.

Proposition 4.1. For $i=1, \dots, r$, the structural energy flows per unit bandwidth $E_i^c(\omega)$, $E_i^d(\omega)$ and $E_i^s(\omega)$ are given by

$$E_i^c(\omega) = -\frac{1}{2\pi} \operatorname{Re}[L(j\omega)(L(j\omega) + Z_s(j\omega))^{-1} S_{w_s w_s}(\omega)(L(j\omega) + Z_s(j\omega))^{-*}]_{(i,i)}, \quad (61)$$

$$E_i^d(\omega) = -\frac{1}{2\pi} \operatorname{Re}[Z_s(j\omega)(L(j\omega) + Z_s(j\omega))^{-1} S_{w_s w_s}(\omega)(L(j\omega) + Z_s(j\omega))^{-*}]_{(i,i)}, \quad (62)$$

$$E_i^s(\omega) = \frac{1}{2\pi} \operatorname{Re}[S_{w_s w_s}(\omega)(L(j\omega) + Z_s(j\omega))^{-*}]_{(i,i)}. \quad (63)$$

In contrast with the case of the modal subsystem model in section 3, $w_i(t)$ and $w_j(t)$ are now mutually uncorrelated for $i \neq j$. (However, these results can be extended to the case in which the structural disturbances are correlated.). Thus by defining the *structural thermodynamic energy* $E_i^{\text{th}}(\omega)$ of the i th structure as

$$E_i^{\text{th}}(\omega) \triangleq \frac{S_{w_i w_i}(\omega)}{2c_i(\omega)}, \quad (64)$$

the following result follows from Theorem 3.2, Corollary 3.3 of reference [27] and the fact that $\operatorname{Re}[L(j\omega)] = 0$.

Proposition 4.2. For $i=1, \dots, r$, $E_i^c(\omega)$ and $E_i^d(\omega)$ are given by

$$E_i^c(\omega) = \sum_{\substack{j=1 \\ j \neq i}}^r \delta_{ij}(\omega) [E_j^{\text{th}}(\omega) - E_i^{\text{th}}(\omega)], \quad (65)$$

$$E_i^d(\omega) = -\delta_{ii}(\omega) E_i^{\text{th}}(\omega) - \sum_{\substack{j=1 \\ j \neq i}}^r \delta_{ij}(\omega) E_j^{\text{th}}(\omega), \quad (66)$$

where, for $i, j = 1, \dots, r$,

$$\delta_{ij}(\omega) \triangleq \frac{1}{\pi} c_i(\omega) c_j(\omega) |[(Z_s(j\omega) + L(j\omega))^{-1}]_{(i,j)}|^2. \quad (67)$$

Equation (65) can be interpreted thermodynamically as saying that energy flow is proportional to thermodynamic energy differences so that energy always flows from higher energy structures to lower energy structures. As shown in reference [27], this result is valid for both weak and strong coupling, unlike predictions based on blocked energy which may be erroneous in the strong coupling case. The validity of equations (65) and (66) is thus due to the use of thermodynamic energy which may be different from stored energy.

Now we consider the structural energy flows. As in the previous section the structural energy flows P_i^c , P_i^d and P_i^e , $i = 1, \dots, r$, are defined by

$$P_i^c \triangleq \int_{-\infty}^{\infty} E_i^c(\omega) d\omega, \quad P_i^d \triangleq \int_{-\infty}^{\infty} E_i^d(\omega) d\omega, \quad (68)$$

$$P_i^e \triangleq \int_{-\infty}^{\infty} E_i^e(\omega) d\omega.$$

The following results correspond to Proposition 3.4.

Proposition 4.3. The structural energy flows per unit bandwidth $E_i^c(\omega)$, $E_i^d(\omega)$, $E_i^e(\omega)$ and the structural energy flows P_i^c , P_i^d , P_i^e satisfy

$$E_i^c(\omega) + E_i^d(\omega) + E_i^e(\omega) = 0, \quad i = 1, \dots, r, \quad (69)$$

$$\sum_{i=1}^r E_i^c(\omega) = 0, \quad (70)$$

$$P_i^c + P_i^d + P_i^e = 0, \quad i = 1, \dots, r, \quad (71)$$

$$\sum_{i=1}^r P_i^c = 0. \quad (72)$$

In the previous section we expressed the modal energy flows P_{ij}^c , P_{ij}^d , P_{ij}^e in terms of the steady-state covariance \tilde{Q}_m according to the approach in reference [27]. To obtain a similar expression for each structure, we must account for the fact that the external disturbance $w(t)$ is no longer white noise and that $c_i(\omega)$ is not constant, in which case the results in reference [27] cannot be applied directly. To overcome these difficulties we introduce the disturbance filter transfer function matrix $T(s)$ defined by

$$T(s) \triangleq \text{diag}(T_1(s), \dots, T_r(s)), \quad (73)$$

and the stable dissipation filter $R_d(s)$ satisfying [35]

$$R_d(s) R_d^T(-s) = C_d(s). \quad (74)$$

By including these filters we consider two augmented systems to obtain P_i^c and P_i^d in equation (68). First let $T(s)$ have the realization

$$\dot{x}_w(t) = A_w x_w(t) + B_w \tilde{w}(t), \quad w_s(t) = C_w x_w(t) + D_w \tilde{w}(t), \quad (75, 76)$$

while the transfer function $Z_s^{-1}(s)$ has the realization

$$\dot{x}_s(t) = A_s x_s(t) + B_s u_s(t), \quad y_s(t) = C_s x_s(t). \quad (77, 78)$$

Furthermore, we define the output matrix C_{ps} for the position vector $x_{ps}(t)$ so that

$$x_{ps}(t) = \int y_s(t) dt = C_{ps} x_s(t). \quad (79)$$

Then by using the stiffness coupling $L(s)$ given by equation (15), we obtain the augmented system

$$\dot{x}_{sa}(t) = \tilde{A}_s x_{sa}(t) + \tilde{D}_s \tilde{w}(t), \quad (80)$$

where

$$x_{sa}(t) \triangleq \begin{bmatrix} x_s(t) \\ x_w(t) \end{bmatrix}, \quad \tilde{A}_s \triangleq \begin{bmatrix} A_s - B_s C_L C_{ps} & B_s C_w \\ 0 & A_w \end{bmatrix},$$

$$\tilde{D}_s \triangleq \begin{bmatrix} B_s D_w \\ B_w \end{bmatrix}.$$

Furthermore, by defining $C_{s1} \triangleq [C_s \ 0]$ and $C_{s2} \triangleq [C_L C_{ps} \ 0]$, it follows that $y_s(t) = C_{s1} x_{sa}(t)$ and $v_s(t) = C_{s2} x_{sa}(t)$.

Next let $R_d(s)$ have the realization

$$\dot{x}_R(t) = A_R x_R(t) + B_R y_s(t), \quad y_R(t) = C_R x_R(t) + D_R y_s(t). \quad (81, 82)$$

Then equations (75)–(79), (81) and (82) yield the augmented system

$$\dot{x}_{da}(t) = \tilde{A}_d x_{da}(t) + \tilde{D}_d \tilde{w}(t), \quad (83)$$

where

$$x_{da}(t) \triangleq \begin{bmatrix} x_s(t) \\ x_w(t) \\ x_R(t) \end{bmatrix},$$

$$\tilde{A}_d \triangleq \begin{bmatrix} A_s - B_s C_L C_{ps} & B_s C_w & 0 \\ 0 & A_w & 0 \\ B_R C_{ps} & 0 & A_R \end{bmatrix},$$

$$\tilde{D}_d \triangleq \begin{bmatrix} B_s D_w \\ B_w \\ 0 \end{bmatrix}.$$

Furthermore, by defining $C_{da} \triangleq [D_R C_{s1} \ C_R]$, it follows that $y_R(t) = C_{da} x_{da}(t)$. With these augmented systems we have the following result.

Theorem 4.1. For, $i = 1, \dots, r$, the structural energy flows P_i^c , P_i^d and P_i^e are given by

$$P_i^c = -(C_{s2} \tilde{Q}_s C_{s1}^T)_{(i,i)}, \quad P_i^d = -(C_{da} \tilde{Q}_d C_{da}^T)_{(i,i)}, \quad (84, 85)$$

and

$$P_i^e = -(C_{s2}\tilde{Q}_s C_{s1}^T + C_{da}\tilde{Q}_d C_{da}^T)_{(i,i)}, \quad (86)$$

where the steady-state covariances $\tilde{Q}_s \triangleq \lim_{t \rightarrow \infty} \mathcal{E}[x_{sa}(t)x_{sa}^T(t)]$ and $\tilde{Q}_d \triangleq \lim_{t \rightarrow \infty} \mathcal{E}[x_{da}(t)x_{da}^T(t)]$ satisfy the algebraic Lyapunov equations

$$0 = \tilde{A}_s \tilde{Q}_s + \tilde{Q}_s \tilde{A}_s^T + \tilde{D}_s \tilde{D}_s^T, \quad 0 = \tilde{A}_d \tilde{Q}_d + \tilde{Q}_d \tilde{A}_d^T + \tilde{D}_d \tilde{D}_d^T. \quad (87, 88)$$

In the following section, we investigate the relation between the modal subsystem model and the structural subsystem model.

5. MODAL COHERENCE EFFECTS IN MODAL AND STRUCTURAL SUBSYSTEM MODELS

In the previous two sections we introduced two energy flow models, namely, the modal subsystem model and the structural subsystem model. Since now each mode is excited by mutually correlated disturbance forces, modal coherence effects play a key role in the relationship between these models.

First, for $i=1, \dots, r$, we define the *total modal coupling, dissipative, and external energy flows* for the i th structure by

$$\mathcal{P}_i^c \triangleq \sum_{j=1}^{n_i} P_{ij}^c, \quad \mathcal{P}_i^d \triangleq \sum_{j=1}^{n_i} P_{ij}^d, \quad \mathcal{P}_i^e \triangleq \sum_{j=1}^{n_i} P_{ij}^e. \quad (89)$$

Note that \mathcal{P}_i^c is the sum of the energy flows through the coupling to all n_i modes of the i th structure, while \mathcal{P}_i^d and \mathcal{P}_i^e can be interpreted in a similar manner. Then, from equations (51) and (52) it follows that

$$\mathcal{P}_i^c + \mathcal{P}_i^d + \mathcal{P}_i^e = 0, \quad \sum_{i=1}^r \mathcal{P}_i^c = 0. \quad (90)$$

Now, concerning \mathcal{P}_i^c , \mathcal{P}_i^d and \mathcal{P}_i^e we obtain the following result.

Theorem 5.1. For $i=1, \dots, r$, the structural and total modal coupling, dissipative, and external energy flows satisfy

$$P_i^c = \mathcal{P}_i^c, \quad P_i^d - \mathcal{P}_i^d = \hat{P}_i, \quad P_i^e - \mathcal{P}_i^e = -\hat{P}_i, \quad (91-93)$$

where

$$\hat{P}_i \triangleq \left[\sum_{j=1}^{n_i} (C_{md} C_{m1} \tilde{Q}_m C_{m1}^T)_{ijij} \right] - (C_{da} \tilde{Q}_d C_{da}^T)_{(i,i)}, \quad (94)$$

and where \tilde{Q}_m and \tilde{Q}_d satisfy equations (48) and (88), respectively.

Proof. From the definition of P_i^c in equation (68) it follows that

$$P_i^c = -\mathcal{E}[y_i(t)v_i(t)] = -\mathcal{E} \left[\sum_{j=1}^{n_i} b_{ij} \dot{q}_{ij}(t) v_i(t) \right] = \sum_{j=1}^{n_i} P_{ij}^c = \mathcal{P}_i^c,$$

which proves equation (91). Equation (92) follows from equations (46) and (85), while equation (93) can be obtained from equations (71), (90), (91) and (92). \square

Theorem 5.1 shows that the energy entering the i th structure through the coupling is equal to the total energy flow received by the n_i modes of the i th structure, while P_i^d and P_i^e are generally different from the sum of the modal energy flows \mathcal{P}_i^d and \mathcal{P}_i^e because of correlation among modes, that is, modal coherence. The following result considers a special case in which the effect of modal coherence disappears so that the structural and total modal dissipative and external energy flows are the same.

Proposition 5.1. Consider the modal coefficients a_{ij} , b_{ij} defined by equations (7)–(9). If

$$a_{ij}/b_{ij} = a_{ik}/b_{ik}, \quad i = 1, \dots, r, \quad j, k = 1, \dots, n_i, \quad (95)$$

then, for $i = 1, \dots, r$,

$$P_i^d = \mathcal{P}_i^d, \quad P_i^e = \mathcal{P}_i^e. \quad (96, 97)$$

Proof. From equations (53) and (54) it follows that

$$w_i = T_i(s)\tilde{w}_i = z_i(s) \sum_{j=1}^{n_i} \frac{a_{ij}b_{ij}}{z_{ij}(s)} \tilde{w}_i = \left(\sum_{j=1}^{n_i} \frac{b_{ij}^2}{z_{ij}(s)} \right)^{-1} \frac{a_{ij}}{b_{ij}} \sum_{j=1}^{n_i} \frac{b_{ij}^2}{z_{ij}(s)} \tilde{w}_i = \frac{a_{ij}}{b_{ij}} \tilde{w}_i.$$

Then, using equations (10) and (11), we have

$$P_i^e = \mathcal{E}[w_i(t)y_i(t)] = \mathcal{E}\left[\frac{a_{ij}}{b_{ij}}\tilde{w}_i(t)y_i(t)\right] = \sum_{j=1}^{n_i} \mathcal{E}[a_{ij}\tilde{w}_i(t)\dot{q}_{ij}(t)] = \mathcal{P}_i^e,$$

which proves equation (97). Equation (96) follows from equations (90), (91) and (97). \square

Assumption (95) holds for the case in which the disturbance location and coupling point coincide for each structure, that is, $\hat{\xi}_i = \xi_{c_i}$.

Now we consider the effect of modal coherence on P_{ij}^e and P_{ij}^d .

Lemma 5.1. For $i = 1, \dots, r$ and $j = 1, \dots, n_i$, the modal coupling and dissipative energy flows P_{ij}^e and P_{ij}^d satisfy

$$P_{ij}^e = -(C_{m2}\tilde{Q}_{\text{Inc}}C_{m1}^T)_{ijj} - \hat{P}_{\text{Coh},ij} \quad (98)$$

and

$$P_{ij}^d = -(C_{m1}C_{m1}\tilde{Q}_{\text{Inc}}C_{m1}^T)_{ijj} + \hat{P}_{\text{Coh},ij}, \quad (99)$$

where

$$\hat{P}_{\text{Coh},ij} \triangleq (C_{m2}\tilde{Q}_{\text{Coh}}C_{m1}^T)_{ijj}, \quad (100)$$

and \tilde{Q}_{Inc} and \tilde{Q}_{Coh} satisfy

$$0 = \tilde{A}_m\tilde{Q}_{\text{Inc}} + \tilde{Q}_{\text{Inc}}\tilde{A}_m^T + \text{Inc}[S_{w_m w_m}], \quad (101)$$

$$0 = \tilde{A}_m\tilde{Q}_{\text{Coh}} + \tilde{Q}_{\text{Coh}}\tilde{A}_m^T + \text{Coh}[S_{w_m w_m}], \quad (102)$$

respectively.

The proof is given in Appendix B. \square

Next we rewrite equations (98) and (99) in terms of the modal thermodynamic energies.

Theorem 5.2. For $i = 1, \dots, r$ and $j = 1, \dots, n_i$, the modal coupling energy flow P_{ij}^c in equation (98) and the modal energy dissipation rate P_{ij}^d in equation (99) are given by

$$P_{ij}^c = \sum_{k=1}^{n_i} \sigma_{ijk} (E_{ik}^{\text{th}} - E_{ij}^{\text{th}}) + \sum_{\substack{p=1 \\ p \neq i}}^r \sum_{q=1}^{n_p} \sigma_{ijpq} (E_{pq}^{\text{th}} - E_{ij}^{\text{th}}) - \hat{P}_{\text{Coh},ij}, \quad (103)$$

$$P_{ij}^d = -\sigma_{ij} E_{ij}^{\text{th}} + \hat{P}_{\text{Coh},ij}, \quad (104)$$

where, for $i, p = 1, \dots, r$, $j = 1, \dots, n_i$, and $q = 1, \dots, n_p$, σ_{ijpq} and σ_{ij} are defined by

$$\sigma_{ijpq} \triangleq \int_{-\infty}^{\infty} \delta_{ijpq}(\omega) d\omega = 2c_{ij} c_{pq} (C_{m1} \tilde{Q}_{pq} C_{m1}^T)_{ijj}, \quad (105)$$

$$\sigma_{ij} \triangleq \sum_{p=1}^r \sum_{q=1}^{n_p} \sigma_{ijpq} \frac{E_{pq}^{\text{th}}}{E_{ij}^{\text{th}}}, \quad (106)$$

and where $\delta_{ijpq}(\omega)$ is defined by equation (37) and \tilde{Q}_{pq} satisfies the Lyapunov equation

$$0 = \tilde{A}_m \tilde{Q}_{pq} + \tilde{Q}_{pq} \tilde{A}_m^T + B_m e_{n_{pq}} e_{n_{pq}}^T B_m^T. \quad (107)$$

Proof. Since $L(s)$ has zero real part, equations (103) and (104) follow from Theorem 4.2 and Corollary 4.2 of reference [27]. Equations (105)–(107) can be obtained directly from Proposition 4.5 of reference [27]. \square

The coefficients σ_{ijpq} in equation (105) and σ_{ij} in equation (106) are called the *modal coupling loss factor* and the *modal internal loss factor*, respectively. It should be noted that $\sigma_{ijpq} = \sigma_{pqij}$ since $L(s)$ is symmetric (see Corollary 4.2 of reference [27]).

We now characterize the energy flows for each structure in terms of the *total modal thermodynamic energy* $\mathcal{E}_i^{\text{th}}$ of the i th structure defined by

$$\mathcal{E}_i^{\text{th}} \triangleq \sum_{j=1}^{n_i} E_{ij}^{\text{th}}. \quad (108)$$

Note that $\mathcal{E}_i^{\text{th}}$ is the sum of the modal thermodynamic energies E_{ij}^{th} of the individual modes of the i th structure. However, because of correlation effects, $\mathcal{E}_i^{\text{th}}$ is generally not equal to the thermodynamic energy E_i^{th} of the i th structure defined by equation (64).

Theorem 5.3. For $i = 1, \dots, r$, the total coupling and dissipative energy flows \mathcal{P}_i^c and \mathcal{P}_i^d satisfy

$$\mathcal{P}_i^c = \sum_{p=1}^r (\eta_{ip} \mathcal{E}_p^{\text{th}} - \eta_{pi} \mathcal{E}_i^{\text{th}}) - \hat{\mathcal{P}}_{\text{Coh},i}, \quad (109)$$

$$\mathcal{P}_i^d = -\eta_i \mathcal{E}_i^{\text{th}} + \hat{\mathcal{P}}_{\text{Coh},i}, \quad (110)$$

where

$$\hat{\mathcal{P}}_{\text{Coh},i} \triangleq \sum_{j=1}^{n_i} \hat{P}_{\text{Coh},ij}, \quad (111)$$

$$\eta_{ip} \triangleq \sum_{q=1}^{n_p} \sum_{j=1}^{n_i} \phi_{pq} \sigma_{ipq}, \quad \eta_i \triangleq \sum_{j=1}^{n_i} \phi_{ij} \sigma_{ij}, \quad (112)$$

and where

$$\phi_{ij} \triangleq \frac{E_{ij}^{\text{th}}}{\mathcal{E}_i^{\text{th}}}. \quad (113)$$

The proof is given in Appendix C.

As in SEA, the coefficients η_{ip} and η_i are called the *coupling loss factor* and the *internal loss factor*, respectively. Note that the weighting factors ϕ_{ij} are non-negative and satisfy

$$\sum_{j=1}^{n_i} \phi_{ij} = 1.$$

Thus the coupling loss factor η_{ip} is a convex combination of the modal coupling loss factors σ_{ipq} and likewise for the internal loss factor η_i .

Remark 5.1. Since $\sum_{j=1}^{n_i} \sum_{k=1}^{n_i} \sigma_{ijk} (E_{ik}^{\text{th}} - E_{ij}^{\text{th}}) = 0$, it follows that the energy flow among different modes of the same structure does not contribute to the total modal coupling energy flow \mathcal{P}_i^{c} . Therefore, it is only necessary to consider energy flow among the modes of different structures.

6. ANALYSIS OF MODAL PAIRWISE INTERACTION

In the previous section we showed that energy flow can be expressed as a linear combination of the modal thermodynamic energies E_{ij}^{th} in equation (103) or total modal thermodynamic energy $\mathcal{E}_i^{\text{th}}$ in equation (109). Our goal in this section is to simplify the results of Theorem 5.3 by decomposing the structural coupling coefficient η_{ip} and dissipative coefficient η_i into pairwise modal interaction terms along with error terms.

To simplify the development we define $x_m(t)$ in equation (40) by

$$x_m(t) \triangleq [\alpha_{11}(t) \quad \beta_{11}(t) \quad \alpha_{12}(t) \quad \beta_{12}(t) \cdots \alpha_{m_r}(t) \quad \beta_{m_r}(t)]^T, \quad (114)$$

where the *energy co-ordinates* are defined by

$$\alpha_{ij}(t) \triangleq \omega_{ij} q_{ij}(t), \quad \beta_{ij}(t) \triangleq \dot{q}_{ij}(t). \quad (115)$$

With this representation for $x_m(t)$, A_m and B_m in equation (40) are given by

$$A_m \triangleq \text{block-diag}(A_{m[11]}, A_{m[12]}, \dots, A_{m[m_r]}),$$

$$B_m \triangleq \text{block-diag}\left(\begin{bmatrix} 0 \\ 1 \end{bmatrix}, \dots, \begin{bmatrix} 0 \\ 1 \end{bmatrix}\right), \quad (116)$$

where $A_{m[ij]}$ denotes the 2×2 matrix

$$A_{m[ij]} = \begin{bmatrix} 0 & \omega_{ij} \\ -\omega_{ij} & -2\zeta_i \omega_{ij} \end{bmatrix}. \quad (117)$$

For the j th mode of the i th structure and the q th mode of the p th structure we decompose $\tilde{A}_m = A_m - \mathcal{A}$ in equation (43) as

$$\tilde{A}_m = \bar{A}^{ipq} - \hat{A}^{ipq}, \quad (118)$$

where

$$\bar{A}^{ipq} \triangleq A_m - \mathcal{A}^{ipq}, \quad \hat{A}^{ipq} \triangleq \mathcal{A} - \mathcal{A}^{ipq}, \quad \mathcal{A} \triangleq B_m E_m C_L E_m^T C_{pm}, \quad (119-121)$$

and

$$\mathcal{A}^{ipq} \triangleq \begin{bmatrix} 0 & \cdots & 0 & 0 & 0 & \cdots & 0 & 0 & 0 & \cdots & 0 \\ \vdots & \vdots & \vdots & \vdots & \vdots & \vdots & \vdots & \vdots & \vdots & \vdots & \vdots \\ 0 & \cdots & 0 & 0 & 0 & \cdots & 0 & 0 & 0 & \cdots & 0 \\ 0 & \cdots & 0 & \mathcal{A}_{[ij]} & 0 & \cdots & 0 & \mathcal{A}_{[ijpq]} & 0 & \cdots & 0 \\ 0 & \cdots & 0 & 0 & 0 & \cdots & 0 & 0 & 0 & \cdots & 0 \\ \vdots & \vdots & \vdots & \vdots & \vdots & \vdots & \vdots & \vdots & \vdots & \vdots & \vdots \\ 0 & \cdots & 0 & \mathcal{A}_{[pqij]} & 0 & \cdots & 0 & \mathcal{A}_{[pq]} & 0 & \cdots & 0 \\ 0 & \cdots & 0 & 0 & 0 & \cdots & 0 & 0 & 0 & \cdots & 0 \\ \vdots & \vdots & \vdots & \vdots & \vdots & \vdots & \vdots & \vdots & \vdots & \vdots & \vdots \\ 0 & \cdots & 0 & 0 & 0 & \cdots & 0 & 0 & 0 & \cdots & 0 \end{bmatrix}, \quad (122)$$

where $\mathcal{A}_{[ijpq]}$ denotes the (n_{ij}, n_{pq}) th 2×2 subblock of \mathcal{A} located at the same position in \mathcal{A}^{ipq} . It can be seen that the decomposition (118) isolates those terms that govern pairwise modal interactions. With this notation we obtain the following result.

Corollary 6.1. The coupling coefficient σ_{ipq} defined by equation (105) is given by

$$\sigma_{ipq} = \bar{\sigma}_{ipq} + \hat{\sigma}_{ipq}, \quad (123)$$

where

$$\bar{\sigma}_{ijj} \triangleq \frac{c_{ij}^2 [\kappa_{ij}^2 (c_{ij} + c_{pq}) + c_{pq} [(\omega_{c,ij}^2 - \omega_{c,pq}^2)^2 + (c_{ij} + c_{pq})(c_{ij}\omega_{c,pq}^2 + c_{pq}\omega_{c,ij}^2)]]}{\kappa_{ij}^2 (c_{ij} + c_{pq})^2 + c_{ij}c_{pq} [(\omega_{c,ij}^2 - \omega_{c,pq}^2)^2 + (c_{ij} + c_{pq})(c_{ij}\omega_{c,pq}^2 + c_{pq}\omega_{c,ij}^2)]}, \quad (124)$$

for $i = 1, \dots, r, j = 1, \dots, n_i$;

$$\bar{\sigma}_{ipq} \triangleq \frac{\kappa_{ij}^2 c_{ij} c_{pq} (c_{ij} + c_{pq})}{\kappa_{ij}^2 (c_{ij} + c_{pq})^2 + c_{ij}c_{pq} [(\omega_{c,ij}^2 - \omega_{c,pq}^2)^2 + (c_{ij} + c_{pq})(c_{ij}\omega_{c,pq}^2 + c_{pq}\omega_{c,ij}^2)]}, \quad (125)$$

for $i \neq p$ or $j \neq q$; and, for $i, p = 1, \dots, r, j = 1, \dots, n_i, q = 1, \dots, n_p$,

$$\hat{\sigma}_{ipq} \triangleq -2c_{ij}c_{pq} (C_{m1} \hat{Q}^{ipq} C_{m1}^T)_{ijj}, \quad (126)$$

where

$$\kappa_{ij}^2 \triangleq K_{ip} b_{ij} b_{pq}, \quad \omega_{c,ij}^2 \triangleq \omega_{ij}^2 + b_{ij}^2 \sum_{\substack{m=1 \\ m \neq i}}^r K_{mi}, \quad (127)$$

and \hat{Q}^{ipq} satisfies

$$0 = \bar{A}^{ipq} \hat{Q}^{ipq} + \hat{Q}^{ipq} \bar{A}^{ipqT} + V^{ipq}, \quad (128)$$

$$V^{ipq} \triangleq \hat{A}^{ipq} \tilde{Q}_{pq} + \tilde{Q}_{pq} \hat{A}^{ipqT}, \quad (129)$$

where \tilde{Q}_{pq} is given by equation (107).

The proof is given in Appendix D.

Remark 6.1. The pairwise modal coupling loss factor $\bar{\sigma}_{ijpq}$ in equation (125) has the same form as the coupling coefficient for the two interconnected oscillators considered in example 1 of reference [27]. Additionally, $\lim_{\kappa_{ip} \rightarrow 0} \bar{\sigma}_{ijpq} = c_{ij}$, that is, $\bar{\sigma}_{ijpq}$ in equation (124) converges to the damping coefficient of the uncoupled mode.

Remark 6.2 Since $\sigma_{ijpq} = \sigma_{pqij}$ and $\bar{\sigma}_{ijpq} = \bar{\sigma}_{pqij}$, it follows that $\hat{\sigma}_{ijpq} = \hat{\sigma}_{pqij}$. As in Corollary 6.1, the modal internal loss factor σ_{ij} in equation (106) can be decomposed as

$$\sigma_{ij} = \bar{\sigma}_{ij} + \hat{\sigma}_{ij}, \quad (130)$$

where

$$\bar{\sigma}_{ij} \triangleq \sum_{p=1}^r \sum_{q=1}^{n_p} \bar{\sigma}_{ijpq} \frac{E_{pq}^{\text{th}}}{E_{ij}^{\text{th}}}, \quad \hat{\sigma}_{ij} \triangleq \sum_{p=1}^r \sum_{q=1}^{n_p} \hat{\sigma}_{ijpq} \frac{E_{pq}^{\text{th}}}{E_{ij}^{\text{th}}}. \quad (131)$$

With this notation P_{ij}^c in equation (103) and P_{ij}^d in equation (104) can be expressed as

$$\begin{aligned} P_{ij}^c &= \sum_{k=1}^{n_i} \bar{\sigma}_{ijk} (E_{ik}^{\text{th}} - E_{ij}^{\text{th}}) + \sum_{\substack{p=1 \\ p \neq i}}^r \sum_{q=1}^{n_p} \bar{\sigma}_{ijpq} (E_{pq}^{\text{th}} - E_{ij}^{\text{th}}) \\ &+ \sum_{k=1}^{n_i} \hat{\sigma}_{ijk} (E_{ik}^{\text{th}} - E_{ij}^{\text{th}}) + \sum_{\substack{p=1 \\ p \neq i}}^r \sum_{q=1}^{n_p} \hat{\sigma}_{ijpq} (E_{pq}^{\text{th}} - E_{ij}^{\text{th}}) - \hat{P}_{\text{Coh},ij}, \end{aligned} \quad (132)$$

$$P_{ij}^d = -\bar{\sigma}_{ij} E_{ij}^{\text{th}} - \hat{\sigma}_{ij} E_{ij}^{\text{th}} + \hat{P}_{\text{Coh},ij}. \quad (133)$$

Furthermore, we can decompose the coupling loss factor η_{ip} and the internal loss factor η_i as shown by the following result.

Corollary 6.2 For $i, p = 1, \dots, r$,

$$\eta_{ip} = \bar{\eta}_{ip} + \hat{\eta}_{ip}, \quad \eta_i = \bar{\eta}_i + \hat{\eta}_i, \quad (134)$$

where

$$\bar{\eta}_{ip} \triangleq \sum_{q=1}^{n_p} \sum_{j=1}^{n_i} \phi_{pq} \bar{\sigma}_{ijpq}, \quad \hat{\eta}_{ip} \triangleq \sum_{q=1}^{n_p} \sum_{j=1}^{n_i} \phi_{pq} \hat{\sigma}_{ijpq}, \quad (135)$$

$$\bar{\eta}_i \triangleq \sum_{j=1}^{n_i} \phi_{ij} \bar{\sigma}_{ij}, \quad \hat{\eta}_i \triangleq \sum_{j=1}^{n_i} \phi_{ij} \hat{\sigma}_{ij}, \quad (136)$$

and where ϕ_{ij} is defined by equation (113).

Proof. This result follows immediately by substituting equations (123) and (130) into η_{ip} and η_i in equation (112), respectively. \square

In analogy with $\bar{\sigma}_{ijpq}$, the parameter $\bar{\eta}_{ip}$ can be viewed as a *pairwise coupling loss factor*.

7. BLOCKED ENERGY AND THERMODYNAMIC ENERGY

In the previous sections we derived energy flow relations involving the modal thermodynamic energy E_{ij}^{th} defined by equation (33). The SEA approach, however, considers the steady-state *blocked modal energy* [1,2,16,31] defined by

$$E_{ij}^{\text{bl}} \triangleq \frac{1}{2} \omega_{c,ij}^2 \mathcal{E}[q_{ij}^2(t)] + \frac{1}{2} \mathcal{E}[\dot{q}_{ij}^2(t)], \quad (137)$$

where $\omega_{c,ij}^2$ is defined by equation (127). As in example 1 of reference [27], the goal of this section is to quantify the distinction between blocked modal energy and modal thermodynamic energy in predicting energy flow.

For convenience, we define the difference \hat{E}_{ij} between the modal thermodynamic energy and the blocked modal energy by

$$\hat{E}_{ij} \triangleq E_{ij}^{\text{th}} - E_{ij}^{\text{bl}}, \quad (138)$$

which is characterized by the following result.

Theorem 7.1. For $i=1, \dots, r$ and $j=1, \dots, n_i$, \hat{E}_{ij} is given by

$$\hat{E}_{ij} = \frac{1}{2} \left[\begin{array}{c} b_{ij}^2 \sum_{p=1}^r K_{ip} \\ \hat{Q}_{(2n_{ij}-1, 2n_{ij}-1)} + \hat{Q}_{(2n_{ij}, 2n_{ij})} - \frac{p \neq i}{\omega_{ij}^2} \tilde{Q}_{m(2n_{ij}, 2n_{ij})} \end{array} \right], \quad (139)$$

where \tilde{Q}_m satisfies equation (48) and \hat{Q} satisfies

$$0 = A_m \hat{Q} + \hat{Q} A_m^T + \hat{V}, \quad (140)$$

where $\hat{V} \triangleq \mathcal{A} \tilde{Q}_m + \tilde{Q}_m \mathcal{A}^T$ and A_m and \mathcal{A} are defined by equations (116) and (121).

The proof is given in Appendix E.

On the other hand, by ignoring the connecting stiffnesses in equation (127) and replacing $\omega_{c,ij}$ by ω_{ij} in the definition of the blocked modal energy, we define the steady-state *uncoupled modal energy* by

$$E_{ij}^{\text{u}} \triangleq \frac{1}{2} \omega_{ij}^2 \mathcal{E}[q_{ij}^2(t)] + \frac{1}{2} \mathcal{E}[\dot{q}_{ij}^2(t)].$$

Proposition 7.1. For $i, m=1, \dots, r$ and $j=1, \dots, n_i$,

$$E_{ij}^{\text{th}} = E_{ij}^{\text{u}}. \quad (141)$$

Proof. The result is obtained by replacing $\omega_{c,ij}$ by ω_{ij} in equation (198) in Appendix E and comparing to equation (197). \square

Proposition 7.1 shows that if the intensity of the disturbance entering each mode and the modal damping coefficient are known, then one can calculate via equation (32) the modal thermodynamic energy and thus the uncoupled modal energy. Note that the definition of the uncoupled modal energy involves the modal displacements and velocities of the *actual* coupled system. Thus, Theorem 5.2 implies that energy flows according to the uncoupled modal energy, that is,

$$P_{ij}^c = \sum_{k=1}^{n_i} \sigma_{ijk} (E_{ik}^u - E_{ij}^u) + \sum_{\substack{p=1 \\ p \neq i}}^r \sum_{q=1}^{n_p} \sigma_{ijpq} (E_{pq}^u - E_{ij}^u) - \hat{P}_{\text{Coh},ij}. \quad (142)$$

SEA, however, is based upon energy flow analysis involving two interconnected oscillators and thus effectively assumes that only one pair of modes is vibrating, while all other modes are fixed or blocked. Thus the blocked modal energy E_{ij}^{bl} is considered in the SEA approach, which inevitably incurs errors due to the difference \hat{E}_{ij} between the modal thermodynamic energy and the blocked modal energy. These error terms are characterized in the following section.

8. FUNDAMENTAL RELATIONS OF STATISTICAL ENERGY ANALYSIS

In the previous three sections we identified error terms due to modal coherence \hat{P}_i and $\hat{\mathcal{P}}_{\text{Coh},i}$, pairwise interaction $\hat{\eta}_{ip}$, and the difference \hat{E}_{ij} between the modal thermodynamic energy and the blocked modal energy. In this section we derive the fundamental relations that form the basis for the SEA approach. These relations clearly show the form of the error terms that are neglected in practice. First we consider the coupling energy flow \mathcal{P}_i^c ($= P_i^c$). To begin, define the *total blocked modal energy* $\mathcal{E}_i^{\text{bl}}$ of the i th structure as

$$\mathcal{E}_i^{\text{bl}} \triangleq \sum_{j=1}^{n_i} E_{ij}^{\text{bl}}. \quad (143)$$

Theorem 8.1. For $i=1, \dots, r$, the total coupling energy flow \mathcal{P}_i^c is given by

$$\mathcal{P}_i^c = \sum_{p=1}^r (\bar{\eta}_{ip} \mathcal{E}_p^{\text{bl}} - \bar{\eta}_{pi} \mathcal{E}_i^{\text{bl}}) + \hat{\mathcal{P}}_i^{\text{bl}} + \hat{\mathcal{P}}_i^{\text{pw}} - \hat{\mathcal{P}}_{\text{Coh},i}, \quad (144)$$

where $\hat{\mathcal{P}}_{\text{Coh},i}$ is defined by equation (111),

$$\hat{\mathcal{P}}_i^{\text{pw}} \triangleq \sum_{p=1}^r (\hat{\eta}_{ip} \mathcal{E}_p^{\text{th}} - \hat{\eta}_{pi} \mathcal{E}_i^{\text{th}}), \quad \hat{\mathcal{P}}_i^{\text{bl}} \triangleq \sum_{p=1}^r (\bar{\eta}_{ip} \hat{\mathcal{E}}_p - \bar{\eta}_{pi} \hat{\mathcal{E}}_i),$$

$$\hat{\mathcal{E}}_i \triangleq \sum_{j=1}^{n_i} \hat{E}_{ij} = \mathcal{E}_i^{\text{th}} - \mathcal{E}_i^{\text{bl}}. \quad (145-147)$$

Proof. The results follow directly from equations (134)–(136), (138) and Theorem 5.3. \square

Next, energy balance at each structure, that is,

$$-\eta_i \mathcal{E}_i^{\text{th}} + \sum_{p=1}^r (\eta_{ip} \mathcal{E}_p^{\text{th}} - \eta_{pi} \mathcal{E}_i^{\text{th}}) + \mathcal{P}_i^c = 0, \quad (148)$$

yields the following result.

Theorem 8.2. For $i=1, \dots, r$,

$$-\bar{\eta}_i \mathcal{E}_i^{\text{bl}} + \sum_{p=1}^r (\bar{\eta}_{ip} \mathcal{E}_p^{\text{bl}} - \bar{\eta}_{pi} \mathcal{E}_i^{\text{bl}}) + P_i^c = -\hat{P}_i - \hat{P}_i^{\text{pw}} - \hat{P}_i^{\text{bl}}, \quad (149)$$

where \hat{P}_i is defined by equation (94),

$$\hat{P}_i^{\text{pw}} \triangleq -\hat{\eta}_i \mathcal{E}_i^{\text{th}} + \sum_{p=1}^r (\hat{\eta}_{ip} \mathcal{E}_p^{\text{th}} - \hat{\eta}_{pi} \mathcal{E}_i^{\text{th}}), \quad (150)$$

$$\hat{P}_i^{\text{bl}} \triangleq -\bar{\eta}_i \hat{\mathcal{E}}_i + \sum_{p=1}^r (\bar{\eta}_{ip} \hat{\mathcal{E}}_p - \bar{\eta}_{pi} \hat{\mathcal{E}}_i). \quad (151)$$

Proof. This result follows from equations (90), (134)–(136), (138) and Theorem 5.3. \square

Note that equations (148) and (149) do not include the modal coherence term $\hat{\mathcal{P}}_{\text{Coh},i}$ defined by equation (111) since this term is cancelled out when \mathcal{P}_i^{c} and \mathcal{P}_i^{d} are added (see Theorem 5.3).

Equation (149) can be rewritten in matrix form, that is,

$$A \mathcal{E}^{\text{bl}} = P_{\text{e}} + \hat{P} + \hat{P}^{\text{pw}} + \hat{P}^{\text{bl}}, \quad (152)$$

where $\mathcal{E}^{\text{bl}} \triangleq [\mathcal{E}_1^{\text{bl}} \dots \mathcal{E}_r^{\text{bl}}]^{\text{T}}$, $P_{\text{e}} \triangleq [P_1^{\text{e}} \dots P_r^{\text{e}}]^{\text{T}}$, $\hat{P} \triangleq [\hat{P}_1 \dots \hat{P}_r]^{\text{T}}$, $\hat{P}^{\text{pw}} \triangleq [\hat{P}_1^{\text{pw}} \dots \hat{P}_r^{\text{pw}}]^{\text{T}}$, $\hat{P}^{\text{bl}} \triangleq [\hat{P}_1^{\text{bl}} \dots \hat{P}_r^{\text{bl}}]^{\text{T}}$ and the $r \times r$ matrix A is defined by

$$A_{(i,i)} \triangleq \bar{\eta}_i + \sum_{\substack{j=1 \\ j \neq i}}^r \bar{\eta}_{ji}, \quad A_{(i,j)} \triangleq -\bar{\eta}_{ij}.$$

Equation (152) is a compartmental model which shows that energy flow can be expressed as a linear combination of subsystem energy. As usual for compartmental models, A is an M -matrix [36,37].

By ignoring the error terms $\hat{\mathcal{P}}_i^{\text{bl}}$, $\hat{\mathcal{P}}_i^{\text{pw}}$ and $\hat{\mathcal{P}}_{\text{Coh},i}$ in equation (144), it follows that

$$\mathcal{P}_i^{\text{c}} = \sum_{p=1}^r (\bar{\eta}_{ip} \mathcal{E}_p^{\text{bl}} - \bar{\eta}_{pi} \mathcal{E}_i^{\text{bl}}), \quad (153)$$

while ignoring \hat{P} , \hat{P}^{pw} and \hat{P}^{bl} in equation (152) yields

$$A \mathcal{E}^{\text{th}} = P_{\text{e}}. \quad (154)$$

Equations (153) and (154) are the fundamental equations considered in the SEA approach [16].

To obtain additional relations considered in SEA, we define the *average modal thermodynamic energy* \bar{E}_i^{th} as

$$\bar{E}_i^{\text{th}} \triangleq \mathcal{E}_i^{\text{th}} / n_i. \quad (155)$$

Theorem 8.3. The pairwise coupling loss factor $\bar{\eta}_{ip}$ defined by equation (135) is given by

$$\bar{\eta}_{ip} = \frac{1}{n_p} \sum_{q=1}^{n_p} \sum_{j=1}^{n_i} \varphi_{pq} \bar{\sigma}_{ijpq}, \quad (156)$$

where

$$\varphi_{pq} \triangleq E_{pq}^{\text{th}} / \bar{E}_p^{\text{th}}. \quad (157)$$

Furthermore, if

$$E_{pq}^{\text{th}} = \bar{E}_p^{\text{th}}, \quad p = 1, \dots, r, q = 1, \dots, n_p, \quad (158)$$

then

$$n_p \bar{\eta}_{ip} = n_i \bar{\eta}_{pi}, \quad i, p = 1, \dots, r. \quad (159)$$

Proof. From the definition of $\bar{\eta}_{ip}$ in equation (135) it follows that

$$\bar{\eta}_{ip} = \sum_{q=1}^{n_p} \sum_{j=1}^{n_i} \phi_{pq} \bar{\sigma}_{ijpq} = \sum_{q=1}^{n_p} \sum_{j=1}^{n_i} \frac{\phi_{pq}}{n_p} \bar{\sigma}_{ijpq},$$

which proves equation (156). Additionally, if equation (158) holds, then $\phi_{pq} = 1$. Thus, equation (156) yields

$$n_p \bar{\eta}_{ip} = n_i \bar{\eta}_{pi} = \sum_{q=1}^{n_p} \sum_{j=1}^{n_i} \bar{\sigma}_{ijpq}. \quad \square$$

By defining the *modal density* v_i as

$$v_i \triangleq n_i / \Delta\omega, \quad (160)$$

where $\Delta\omega$ is the width of the frequency band in which the $\sum_{i=1}^r n_i$ modes lie, equation (159) can be rewritten as

$$v_p \bar{\eta}_{ip} = v_i \bar{\eta}_{pi}. \quad i, p = 1, \dots, r. \quad (161)$$

In SEA terminology, equations (158) and (161) represent *equipartition of energy* and *reciprocity*, respectively [16].

9. PAIRWISE MODAL COUPLING LOSS FACTOR IN THE WEAK COUPLING CASE

As seen in equation (135), the pairwise coupling loss factor $\bar{\eta}_{ip}$ depends on the pairwise modal coupling loss factor $\bar{\sigma}_{ijpq}$ defined by equation (125). In this section, we consider the weak coupling case and derive an alternative pairwise modal coupling loss factor. In this case, these two pairwise modal coupling loss factors are shown to be approximations of the actual modal coupling loss factor σ_{ijpq} defined by equation (105).

The following result focuses on the size of the modal coupling loss factor as determined by the off-diagonal portion $\langle L(j\omega) \rangle$ of $L(j\omega)$.

Proposition 9.1. Define

$$Z(j\omega) \triangleq Z_m(j\omega) + \{L_m(j\omega)\} \quad (162)$$

and assume that

$$\|Z^{-1}(j\omega)\langle L_m(j\omega) \rangle\| < 1, \quad (163)$$

where $\|\cdot\|$ denotes the spectral norm. Then the modal coupling loss factor σ_{ijpq} defined by equation (105) is given by

$$\sigma_{ijpq} = \tilde{\sigma}_{ijpq} + \frac{c_{ij}c_{pq}}{\pi} \int_{-\infty}^{\infty} \delta_{ijpq}(j\omega) d\omega, \quad (164)$$

where

$$\tilde{\sigma}_{ijpq} \triangleq \frac{\kappa_{ijpq}^2 (c_{ij} + c_{pq})}{(\omega_{c,ij}^2 - \omega_{c,pq}^2)^2 + (c_{ij} + c_{pq})(c_{ij}\omega_{c,pq}^2 + c_{pq}\omega_{c,ij}^2)}, \quad (165)$$

$$\hat{\delta}_{ijpq}(\omega) \triangleq |\mathcal{O}(\omega)_{ijpq}|^2 + 2\operatorname{Re} \left[\frac{\frac{1}{j\omega} \kappa_{ijpq}}{\hat{z}_{ij}(j\omega) \hat{z}_{pq}(j\omega)} \mathcal{O}(\omega)_{ijpq} \right], \quad (166)$$

$$\mathcal{O}(\omega) \triangleq Z^{-1}(j\omega) \sum_{n=2}^{\infty} [-Z^{-1}(j\omega) \langle L_m(j\omega) \rangle]^n, \quad (167)$$

$$\hat{z}_{ij}(s) \triangleq \frac{s^2 + 2\zeta_{ij} \omega_{ij} s + \omega_{c,ij}^2}{s}, \quad (168)$$

and κ_{ijpq} and $\omega_{c,ij}$ are defined by equation (127).

The proof is given in Appendix F.

Proposition 9.1 shows that the pairwise modal coupling loss factor $\tilde{\sigma}_{ijpq}$ given by equation (165) is a first order approximation for σ_{ijpq} in terms of the coupling matrix $L(j\omega)$. The pairwise modal coupling loss factor $\tilde{\sigma}_{ijpq}$ was derived in references [2, 8] for two interconnected oscillators (see example 1 in reference [27]) and plays a central role in SEA. The following result examines the relationship between the pairwise modal coupling loss factors $\tilde{\sigma}_{ijpq}$ and $\bar{\sigma}_{ijpq}$.

Proposition 9.2. Suppose equation (163) holds. Then

$$\tilde{\sigma}_{ijpq} = \bar{\sigma}_{ijpq} - \frac{Q_{ijpq} \bar{\sigma}_{ijpq}^2}{1 + Q_{ijpq} \bar{\sigma}_{ijpq}}, \quad (169)$$

where

$$Q_{ijpq} \triangleq \frac{(c_{ij} + c_{pq})(c_{ij}c_{pq} - \kappa_{ijpq})}{\kappa_{ijpq} c_{ij} c_{pq}}. \quad (170)$$

Proof. The result follows from equations (125) and (165). \square

As can be seen from equations (125) and (165), both $\bar{\sigma}_{ijpq}$ and $\tilde{\sigma}_{ijpq}$ depend on second order terms in K_{ip} , while $Q_{ijpq} \bar{\sigma}_{ijpq}^2 / (1 + Q_{ijpq} \bar{\sigma}_{ijpq})$ in equation (169) depends on fourth order terms in K_{ip} . Thus, $\bar{\sigma}_{ijpq}$ and $\tilde{\sigma}_{ijpq}$ coincide up to quadratic terms in the coupling stiffness. Furthermore, since $\mathcal{O}(\omega)$ in equation (167) depends on terms higher than second order in K_{ip} , it follows that $\hat{\delta}_{ijpq}(j\omega)$ in equation (166) depends on terms higher than third order in K_{ip} . Thus, both $\bar{\sigma}_{ijpq}$ and $\tilde{\sigma}_{ijpq}$ coincide with σ_{ijpq} up to quadratic terms in the coupling stiffness. This result can also be obtained by analyzing the error term $\hat{\sigma}_{ijpq}$ given by equation (126). Consequently, in the weak coupling case it follows that $\sigma_{ijpq} \cong \bar{\sigma}_{ijpq} \cong \tilde{\sigma}_{ijpq}$, that is, both pairwise modal coupling loss factors $\bar{\sigma}_{ijpq}$ and $\tilde{\sigma}_{ijpq}$ are approximations of the modal coupling loss factor σ_{ijpq} .

10. LIMITING RESULTS INVOLVING THE ERROR TERMS

In section 8, we derived equations (144) and (152) involving error terms and showed that except for these error terms the energy flow (153) agrees with results obtained in reference [16]. Since the error terms are generally non-zero, we consider, in this section, limiting results which give conditions under which these terms go to zero. First we consider the error \hat{P}_i defined by equation (94) which arises due to modal coherence. For the following results the notation $\lim_{\kappa_{i\{m\}} \rightarrow 0}$ denotes the index set involved in the limiting procedure.

Proposition 10.1. For $i=1,\dots,r$,

$$\lim_{\substack{K_{i\{m\}} \rightarrow 0 \\ \zeta_{i\{j\}} \rightarrow 0}} \hat{P}_i = 0. \quad (171)$$

The proof is given in Appendix G.

Proposition 10.1 shows that, in the limit $K_{i\{m\}}, \zeta_{i\{j\}} \rightarrow 0$, the discrepancy between energy flow predictions based on the modal subsystem model and predictions based on the structural subsystem model vanishes. At the same time we can obtain the following result.

Proposition 10.2. Let the steady-state modal covariance \tilde{Q}_m satisfy the Lyapunov equation (48). Then

$$\lim_{\substack{K_{i\{m\}} \rightarrow 0 \\ \zeta_{i\{j\}} \rightarrow 0}} E_0^{-1/2} \tilde{Q}_m E_0^{-1/2} = I, \quad (172)$$

where

$$E_0 \triangleq \text{diag}(E_{11}^{\text{th}}, E_{11}^{\text{th}}, E_{12}^{\text{th}}, E_{12}^{\text{th}}, \dots, E_{m_r}^{\text{th}}, E_{m_r}^{\text{th}}). \quad (173)$$

The proof is given in Appendix H.

Next we consider the effect of modal coherence on the coupling energy flow \mathcal{P}_i^c in equation (109).

Proposition 10.3. For $i=1,\dots,r$,

$$\lim_{K_{i\{m\}} \rightarrow 0} \hat{\mathcal{P}}_{\text{Coh},i} = 0. \quad (174)$$

The proof is given in Appendix I.

Propositions 10.1 and 10.2 show that, in the limit $K_{i\{m\}}, \zeta_{i\{j\}} \rightarrow 0$, the steady-state covariance \tilde{Q}_m converges to the diagonal matrix E_0 , which shows that \hat{P}_i vanishes and modal incoherence occurs. Furthermore, Proposition 10.3 shows that $\hat{\mathcal{P}}_{\text{Coh},ij}$ also vanishes as $K_{i\{m\}} \rightarrow 0$, which implies that the structure can be viewed as a set of modes (oscillators) excited by uncorrelated disturbance forces. Thus, in the limiting case of light damping and weak coupling, the structural subsystem model is equivalent to the modal subsystem model in which each mode is excited by an uncorrelated disturbance. This fact has been rigorously verified by Propositions 10.1–10.3.

Next we consider the error term \hat{P}_i^{bl} in equation (151) due to the difference between the blocked modal energy E_{ij}^{bl} and the modal thermodynamic energy E_{ij}^{th} .

Proposition 10.4. For $i=1,\dots,r$,

$$\lim_{K_{i\{m\}} \rightarrow 0} \hat{\mathcal{P}}_i^{\text{bl}} = \lim_{K_{i\{m\}} \rightarrow 0} \hat{P}_i^{\text{bl}} = 0. \quad (175)$$

Proof. Since $\lim_{K_{i\{m\}} \rightarrow 0} \mathcal{A} = 0$, where \mathcal{A} is defined by equation (121), it follows from equations (139) and (140) that $\lim_{K_{i\{m\}} \rightarrow 0} \hat{E}_{ij} = 0$, which proves equation (175). \square

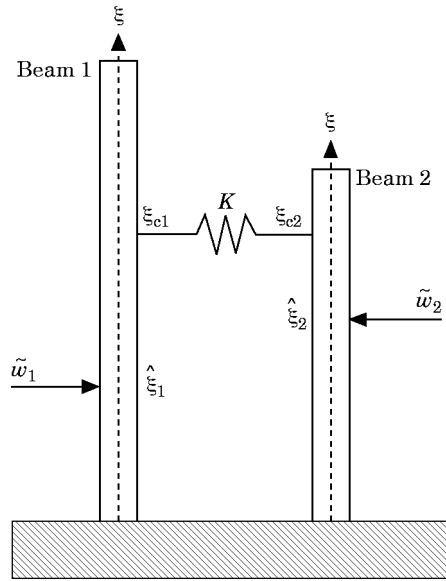


Figure 5. Cantilevered beams interconnected by stiffness coupling.

Proposition 10.4 says that $\lim_{K_{i(m)} \rightarrow 0} E_{ij}^{bl} = E_{ij}^{th}$ so that in the weak coupling case the blocked energy E_{ij}^{bl} can be replaced by the thermodynamic energy E_{ij}^{th} . This approximation does not hold under strong coupling as shown in section 7 of reference [27]. Finally, we obtain a similar result involving the effects of pairwise interaction $\hat{\mathcal{P}}_i^{pw}$ and \hat{P}_i^{pw} .

Proposition 10.5. For $i = 1, \dots, r$,

$$\lim_{K_{i(m)} \rightarrow 0} \hat{\mathcal{P}}_i^{pw} = \lim_{K_{i(m)} \rightarrow 0} \hat{P}_i^{pw} = 0. \tag{176}$$

Proof. As $\lim_{K_{i(m)} \rightarrow 0} \mathcal{A}^{ipq}$ defined by equation (120) converges to zero, which implies V^{ipq} defined by equation (129) also converges to zero. Thus from equation (128), $\lim_{K_{i(m)} \rightarrow 0} \hat{Q}^{ipq} = 0$, which proves equation (176). \square

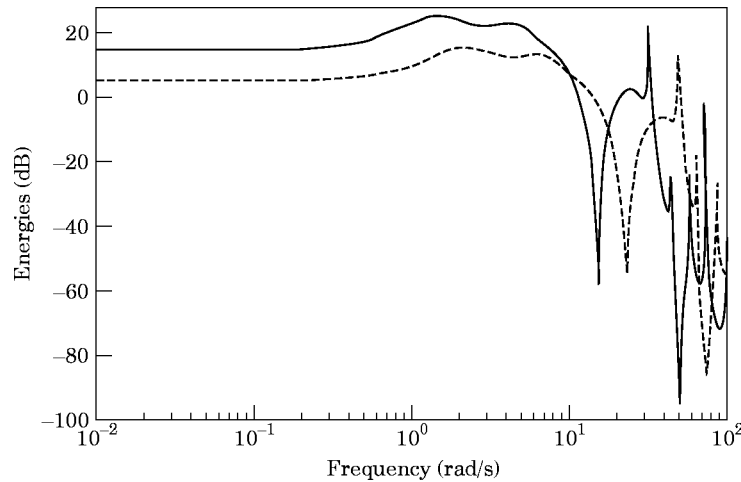


Figure 6. Thermodynamic energies: —, $E_1^{th}(\omega)$; ---, $E_2^{th}(\omega)$.

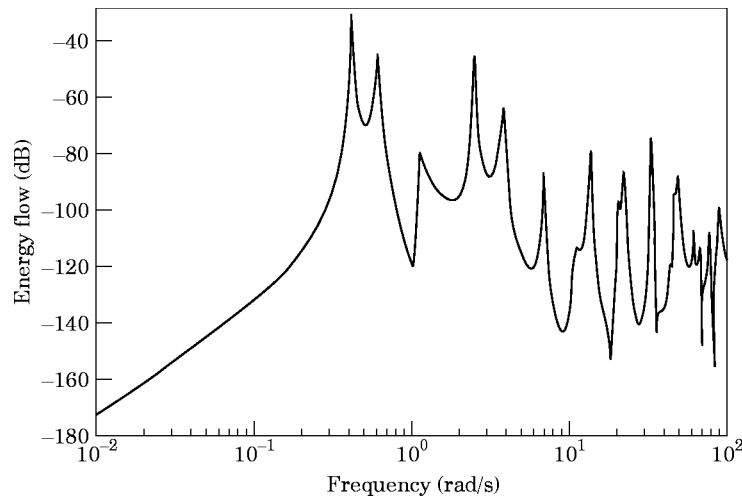


Figure 7. Coupling energy flow: $E_1(\omega)$ and $E_2(\omega)$.

From the results obtained in Propositions 10.3–10.5 we can conclude that if the coupling is sufficiently small then the SEA fundamental equation (153) holds approximately. Additionally, if the coupling and the modal damping are sufficiently small then equation (154) holds approximately according to Propositions 10.1, 10.4 and 10.5. These results are illustrated in the following section by means of a numerical example.

11. NUMERICAL EXAMPLE

As a numerical example we consider interconnected uniform cantilevered beams as shown in Figure 5. The beams are of lengths L_1, L_2 , mass densities ρ_1, ρ_2 , and bending stiffnesses $E_1 I_{A1}, E_2 I_{A2}$, respectively. Each beam is subjected to mutually uncorrelated white noise disturbances $\tilde{w}_i(t)$, $i=1,2$, with unit intensity applied at ξ_i and interconnected by a spring with stiffness K at ξ_{c_i} .

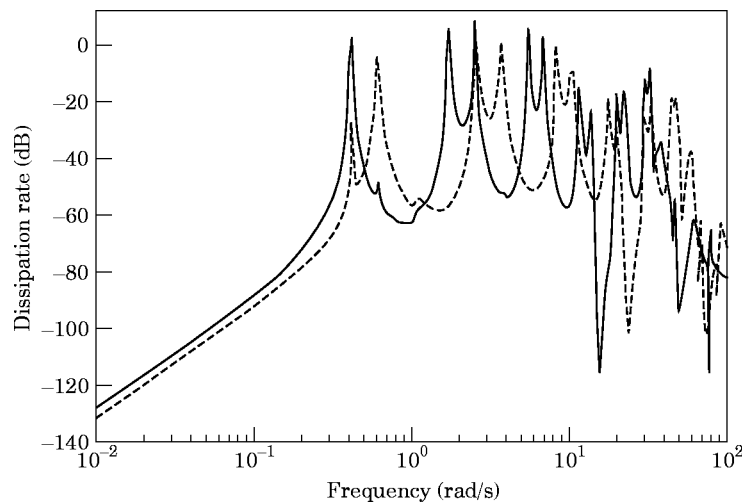


Figure 8. Energy dissipation rate. —, $E_1^d(\omega)$; ---, $E_2^d(\omega)$.

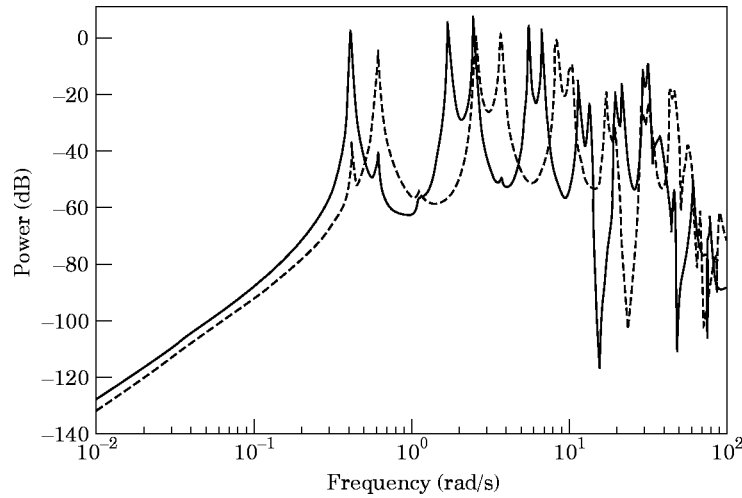


Figure 9. External power: —, $E_1^c(\omega)$; ---, $E_2^c(\omega)$.

By considering the boundary conditions

$$\begin{aligned} \chi_i(\xi, t)|_{\xi=0} &= 0, & \frac{\partial \chi_i(\xi, t)}{\partial \xi} \Big|_{\xi=0} &= 0, & \frac{\partial^2 \chi_i(\xi, t)}{\partial \xi^2} \Big|_{\xi=L_i} &= 0, \\ \frac{\partial^3 \chi_i(\xi, t)}{\partial \xi^3} \Big|_{\xi=L_i} &= 0, & i &= 1, 2, \end{aligned}$$

we obtain the natural frequencies and eigenfunctions as [16]

$$\begin{aligned} \omega_{ij} &= k_{ij}^2 \sqrt{E_i I_{\Lambda_i} / m_i}, \\ \psi_{ij}(\xi_i) &= A_{ij} [(\sin k_{ij} L_i - \sinh k_{ij} L_i)(\sin k_{ij} \xi - \sinh k_{ij} \xi) \\ &\quad + (\cos k_{ij} L_i - \cosh k_{ij} L_i)(\cos k_{ij} \xi - \cosh k_{ij} \xi)], \end{aligned}$$

where A_{ij} is the normalized parameter so that equation (5) holds and the wave number k_{ij} satisfies $\cos k_{ij} L_i \cosh k_{ij} L_i = -1$. Thus, a_{ij} and b_{ij} in equation (6) are given by $a_{ij} = \psi_{ij}(\xi_i)$ and $b_{ij} = \psi_{ij}(\xi_{c_i})$.

We now consider the first 10 modes of beam 1 and the first seven modes of beam 2 so that $n_1 = 10$, $n_2 = 7$. By setting $L_1 = 3$, $L_2 = 2.5$, $\rho_1 = \rho_2 = 1$, $E_1 I_{\Lambda_1} = 1$, $E_2 I_{\Lambda_2} = 1 \cdot 1^2$, $K = 0.01$, $\zeta_{1j} = 0.01$, $\zeta_{2j} = 0.02$, $j = 1, 2, 3$, $\xi_1 = 1$, $\xi_2 = 1.5$ and $\xi_{c_1} = \xi_{c_2} = 2.2$, the steady state energy quantities per unit bandwidth $E_1^{\text{th}}(\omega)$, $E_1^c(\omega)$, $E_1^d(\omega)$ and $E_1^s(\omega)$ are shown in Figures 6–9, respectively. Since the conservation of energy at the coupling, equation (70) of Proposition 4.2, holds, it follows that $E_1^c(\omega) = -E_2^c(\omega)$. Thus, as shown in Figure 7, $E_1^c(\omega)$ and $E_2^c(\omega)$ have the same magnitude.

Next we examine the relationship between the thermodynamic energies $E_1^{\text{th}}(\omega)$, $E_2^{\text{th}}(\omega)$ and the coupling energy flow $E_1^c(\omega)$. Figure 10 shows that if $E_1^{\text{th}}(\omega) > E_2^{\text{th}}(\omega)$ then $E_1^c(\omega) < 0$, that is, energy flows from beam 1 to beam 2, while if $E_1^{\text{th}}(\omega) < E_2^{\text{th}}(\omega)$ then $E_1^c(\omega) > 0$, that is, energy flows from beam 2 to beam 1. This result is predicted by equation (65) of Proposition 4.3.

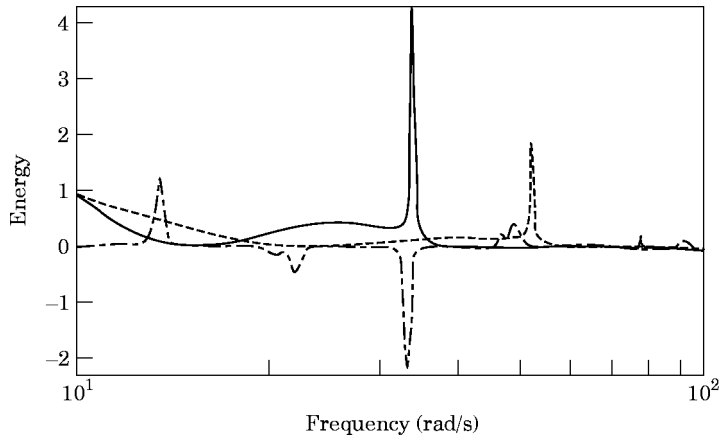


Figure 10. Relationship between thermodynamic energy and coupling energy flow. —, $E_1^{\text{th}}(\omega)$; ---, $E_2^{\text{th}}(\omega)$; — · —, $E_i^{\text{c}}(\omega) \times 5000$.

Next, we examine the convergence of the residual terms considered in the previous section. Consider the first ten modes of beam 1 and the first seven modes of beam 2. Furthermore, define

$$\hat{\mathcal{R}}_i \triangleq \left| \frac{\hat{\mathcal{P}}_{\text{Coh}i}}{\mathcal{P}_i^{\text{p}}} \right|, \quad \hat{R}_i \triangleq \left| \frac{\hat{P}_i}{P_i^{\text{c}}} \right|, \quad i = 1, 2, \quad (177)$$

$$\hat{\mathcal{R}}_i^{\text{pw}} \triangleq \left| \frac{\hat{\mathcal{P}}_i^{\text{pw}}}{\mathcal{P}_i^{\text{p}}} \right|, \quad \hat{R}_i^{\text{pw}} \triangleq \left| \frac{\hat{P}_i^{\text{pw}}}{P_i^{\text{c}}} \right|, \quad i = 1, 2, \quad (178)$$

$$\hat{\mathcal{R}}_i^{\text{bl}} \triangleq \left| \frac{\hat{\mathcal{P}}_i^{\text{bl}}}{\mathcal{P}_i^{\text{p}}} \right|, \quad \hat{R}_i^{\text{bl}} \triangleq \left| \frac{\hat{P}_i^{\text{bl}}}{P_i^{\text{c}}} \right|, \quad i = 1, 2, \quad (179)$$

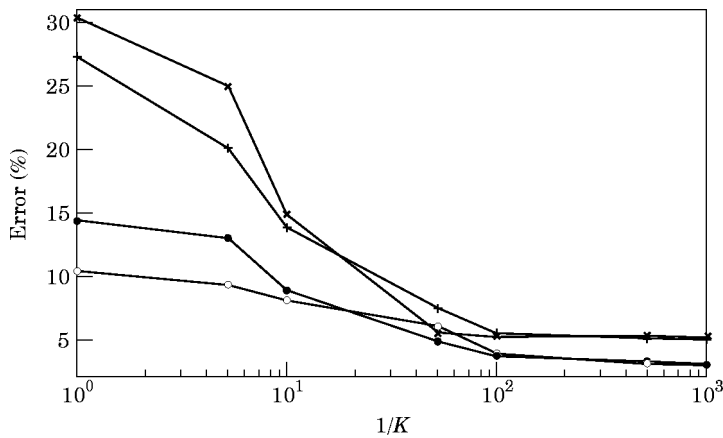


Figure 11. Error terms versus coupling stiffness K . \circ —, $\hat{\mathcal{R}}_1$; $+$ —, $\hat{\mathcal{R}}_1^{\text{pw}}$; $*$ —, $\hat{\mathcal{R}}_1^{\text{bl}}$; \times —, $\hat{\mathcal{R}}_2$.

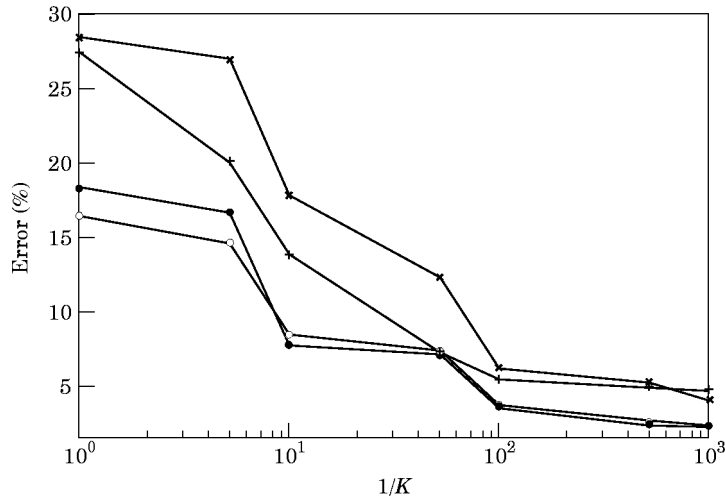


Figure 12. Error terms for beam 1 versus coupling stiffness K . $-\circ-$, \hat{R}_1 ; $+-$, \hat{R}_1^{pw} ; $-*-$, \hat{R}_1^{bl} ; $- \times -$, R_1 .

$$\mathcal{R}_i \triangleq \left| \frac{\hat{\mathcal{P}}_{\text{Coh},i} + \hat{\mathcal{P}}_i^{pw} + \hat{\mathcal{P}}_i^{bl}}{\mathcal{P}_i^e} \right|, \quad R_i \triangleq \left| \frac{\hat{P}_i + \hat{P}_i^{pw} + \hat{P}_i^{bl}}{P_i^e} \right|, \quad i=1,2. \quad (180)$$

According to equations (144) and (149), these quantities are the ratios of the error terms to the exact energy flow value. In particular, \mathcal{R}_i and R_i denote the ratio of total error to the exact energy flow and if $\mathcal{R}_i=0$ and $R_i=0$, then the exact energy flow expressions (144) and (152) converge to equations (153) and (154), respectively.

First we consider the effect of coupling K on the error terms (177)–(180). By setting $\zeta_{ij}=\zeta_{2q}=0.01$, $j=1, \dots, 10$, $q=1, \dots, 7$, we calculate these ratios. Since $\sigma_{ijpq}=\sigma_{pqij}$ and $r=2$ it follows that $\mathcal{P}_1^e = -\mathcal{P}_2^e$, $\hat{\mathcal{P}}_{\text{Coh},1} = -\hat{\mathcal{P}}_{\text{Coh},2}$, $\hat{\mathcal{P}}_1^{pw} = -\hat{\mathcal{P}}_2^{pw}$ and $\hat{\mathcal{P}}_1^{bl} = -\hat{\mathcal{P}}_2^{bl}$. Thus it suffices to examine $\hat{\mathcal{R}}_1$, $\hat{\mathcal{R}}_1^{pw}$, $\hat{\mathcal{R}}_1^{bl}$ and \mathcal{R}_1 . Figure 11 shows that $\hat{\mathcal{R}}_1$ decreases with the coupling stiffness

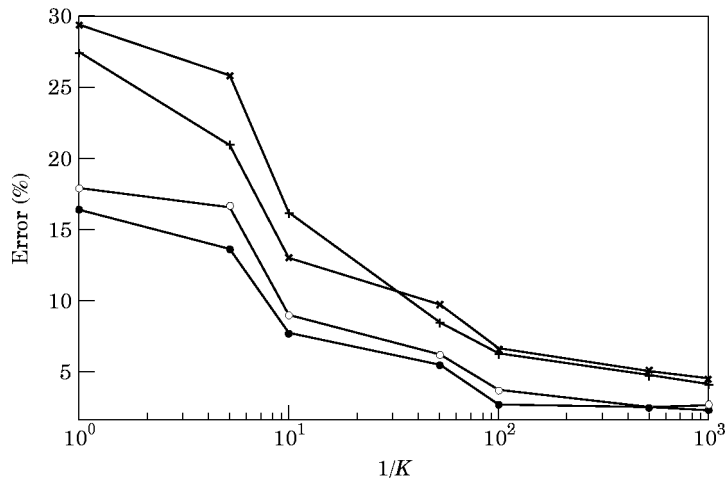


Figure 13. Error terms for beam 2 versus coupling stiffness K . $-\circ-$, \hat{R}_2 ; $+-$, \hat{R}_2^{pw} ; $-*-$, \hat{R}_2^{bl} ; $- \times -$, R_2 .

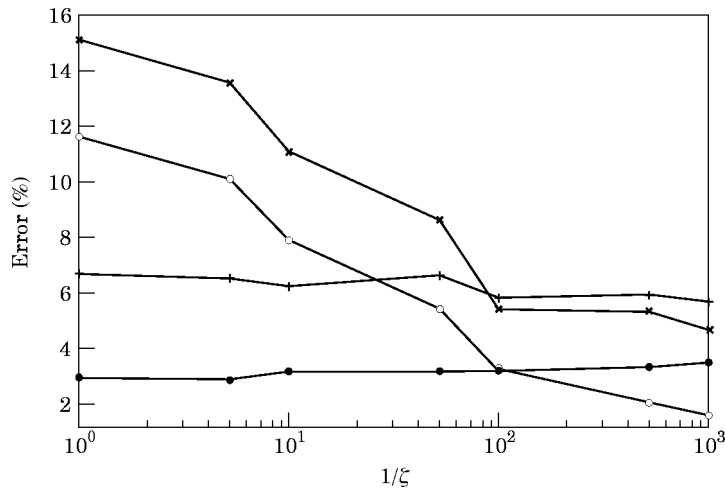


Figure 14. Error terms for beam 1 versus damping ζ . $-\circ-$, \hat{R}_1 ; $-+-$, \hat{R}_1^{pw} ; $-*-$, \hat{R}_1^{bl} ; $-x-$, R_1 .

K as guaranteed by Proposition 10.3, while $\hat{\mathcal{H}}_i^{pw}$ and $\hat{\mathcal{H}}_i^{bl}$ decrease with the coupling stiffness K as guaranteed by Propositions 10.4 and 10.5. Consequently, \mathcal{R}_i decrease with the coupling stiffness. The same analysis can be applied to \hat{R}_i , \hat{R}_i^{pw} , \hat{R}_i^{bl} and R_i , $i = 1, 2$, plotted in Figures 12 and 13. Furthermore, from Figures 11–13 it can be seen that the effect of pairwise interaction $\hat{\mathcal{H}}_i^{pw}$ and \hat{R}_i^{pw} is larger than both effects of modal coherence $\hat{\mathcal{H}}_i$, \hat{R}_i and the difference between the thermodynamic energy and the stored blocked energy $\hat{\mathcal{H}}_i^{bl}$, \hat{R}_i^{bl} .

Now, we consider the effect of damping ζ_{ij} on the residual terms \hat{R}_i , \hat{R}_i^{pw} , \hat{R}_i^{bl} and R_i , $i = 1, 2$. By setting $\zeta_{1j} = \zeta_{2q} = \zeta$, $j = 1, \dots, 10$, $q = 1, \dots, 7$ and $K = 0.01$, Figures 14 and 15 show that \hat{R}_i decreases with the damping ζ as explained by Proposition 10.1.

12. CONCLUSIONS

In this paper we applied the energy flow model obtained in reference [27] to the case of conservatively coupled structures. We obtained two energy flow models, namely, the modal

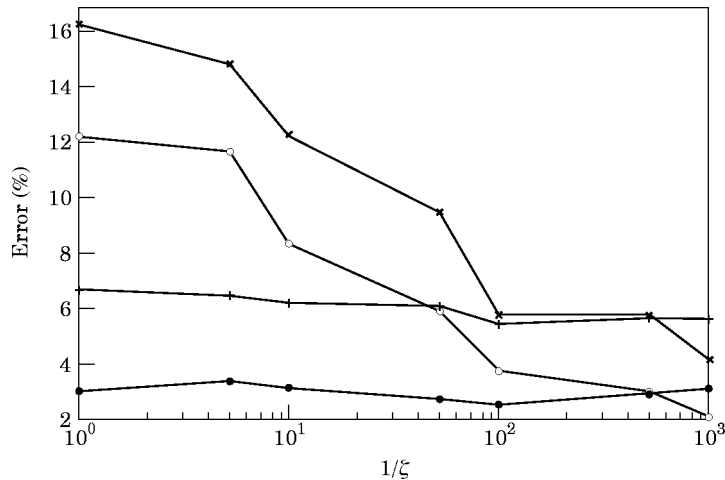


Figure 15. Error terms for beam 2 versus damping ζ . $-\circ-$, \hat{R}_2 ; $-+-$, \hat{R}_2^{pw} ; $-*-$, \hat{R}_2^{bl} ; $-x-$, R_2 .

subsystem model and the structural subsystem model, which predict energy flow among modes or structures. Furthermore, by using these two energy flow models, the fundamental relations that form the basis for SEA were derived along with error terms. The fundamental equation that characterizes the SEA approach is a compartmental model which shows that energy flow can be expressed as a linear combination of subsystem energy, while the error terms arise from the effects of the modal coherence, pairwise interaction and the difference between the thermodynamic energy and the blocked energy. These error terms were shown to become small under weak coupling and light modal damping. These properties, which were demonstrated by means of numerical examples, validate the use of SEA relations in the limiting case and quantify the magnitude of the error in the case of strong coupling.

There are several extensions to this work that warrant investigation. In particular, the case of structures interconnected at multiple points remains to be considered. Furthermore, a comparison with the SEA relations obtained in reference [17] is of interest. Finally, a comparison of these results to ensemble averaging and an investigation of the role of modal overlap remain areas for future research.

ACKNOWLEDGMENTS

We wish to thank Dave Hyland, Wassim Haddad, Matthew Cartmell, Al Kriman, Doug MacMartin, Jonathan How, Scot Osburn, and the anonymous reviewers for numerous helpful discussions and suggestions. This research was supported in part by the Air Force Office of Scientific Research under Grant F49620-92-J-0127 and the NASA SERC Grant NAGW-1335.

REFERENCES

1. R. H. LYON and G. MAIDANIK 1962 *Journal of the Acoustical Society of America* **34**, 623–639. Power flow between linear coupled oscillators.
2. T. D. SCHARTON and R. H. LYON 1968 *Journal of the Acoustical Society of America* **43**, 1332–1343. Power flow and energy sharing in random vibrations.
3. D. E. NEWLAND 1968 *Journal of Sound and Vibration* **3**, 553–559. Calculation of power flow between coupled oscillators.
4. S. R. CRANDALL and R. LOTZ 1971 *Journal of the Acoustical Society of America* **49**, 352–356. On the coupling loss factor in statistical energy analysis.
5. H. G. DAVIES 1972 *Journal of the Acoustical Society of America* **51**, 387–392. Exact solutions for the response of some coupled multimodal systems.
6. H. G. DAVIES 1972 *Journal of the Acoustical Society of America* **51**, 393–401. Power flow between two coupled beams.
7. H. G. DAVIS 1973 *Journal of the Acoustical Society of America* **54**, 507–515. Random vibration of distributed systems strongly coupled at discrete points.
8. R. H. LYON 1975 *Statistical Energy Analysis of Dynamical Systems: Theory and Applications*. Cambridge: MIT Press.
9. G. MAIDANIK 1976 *Journal of Sound and Vibration* **46**, 561–583. Response of coupled dynamic systems.
10. G. MAIDANIK 1977 *Journal of Sound and Vibration* **52**, 171–191. Some elements in statistical energy analysis.
11. P. W. SMITH JR. 1979 *Journal of the Acoustical Society of America* **65**, 695–698. Statistical models of coupled dynamical systems and the transition from weak to strong coupling.
12. J. WOODHOUSE 1981 *Journal of the Acoustical Society of America* **69**, 1695–1709. An approach to the theoretical background of statistical energy analysis applied to structural vibration.
13. F. J. FAHY 1982 *Noise and Vibration* (R. G. White and J. G. Walker, editors), Chapter 7. Chichester, U. K.: Ellis Horwood.
14. C. H. HODGES and J. WOODHOUSE 1986 *Reports on Progress in Physics* **49**, 107–170. Theories of noise and vibration transmission in complex structures.

15. A. J. KEAN and W. G. PRICE 1987 *Journal of Sound and Vibration* **117**, 363–386. Statistical energy analysis of strongly coupled systems.
16. M. P. NORTON 1989 *Foundations of Noise and Vibration Analysis for Engineers*, Cambridge: Cambridge University Press.
17. R. S. LANGLEY 1989 *Journal of Sound and Vibration* **135**, 499–508. A general derivation of the statistical energy analysis equations for coupled dynamic systems.
18. R. S. LANGLEY 1990 *Journal of Sound and Vibration* **141**, 207–219. A derivation of the coupling loss factors used in statistical energy analysis.
19. A. J. KEANE and W. G. PRICE 1990 *Proceedings of the Institute of Acoustics* **12**, 535–542. Exact power flow relationships between many multi-coupled multi-modal subsystems.
20. A. J. KEANE and W. G. PRICE 1991 *Journal of Sound and Vibration* **144**, 185–196. A note on the power flowing between two conservatively coupled multi-modal subsystems.
21. B. R. MACE 1992 *Journal of Sound and Vibration* **154**, 289–320. Power flow between two continuous one-dimensional subsystems: a wave solution.
22. B. R. MACE 1992 *Journal of Sound and Vibration* **159**, 305–327. Power flow between two coupled beams.
23. R. S. LANGLEY 1992 *Journal of Sound and Vibration* **159**, 483–502. A wave intensity technique for the analysis of high frequency vibration.
24. J. PAN, J. PAN and C. H. HANSEN 1992 *Journal of the Acoustical Society of America* **92**, 895–907. Total power flow from a vibrating rigid body to a thin panel through multiple elastic mounts.
25. A. J. KEAN 1993 *Journal of Sound and Vibration* **164**, 143–156. A note on modal summations as applied to statistical energy analysis (S.E.A.).
26. B. R. MACE 1993 *Journal of Sound and Vibration* **166**, 429–461. The statistical energy analysis of two continuous one-dimensional subsystems.
27. Y. KOSHIMOTO and D. S. BERNSTEIN 1994 *Journal of Sound and Vibration* **182**, 23–58. Thermodynamic modelling of interconnected systems: I. conservative coupling.
28. J. L. WYATT, W. M. SIEBERT and H. N. TAN 1984 *IEEE Transactions on Circuits and Systems* **31**, 809–824. A frequency domain inequality for stochastic power flow in linear networks.
29. C. H. HODGES and J. WOODHOUSE 1989 *Journal of Sound and Vibration* **130**, 237–251. Confinement of vibration by one-dimensional disorder, I: theory of ensemble averaging.
30. C. H. HODGES and J. WOODHOUSE 1989 *Journal of Sound and Vibration* **130**, 253–268. Confinement of vibration by one-dimensional disorder, II: a numerical experiment on different ensemble averages.
31. R. H. LYON 1987 *Statistical Energy Analysis, ASME Winter Annual Meeting, Boston, MA*, December, p. 1. The SEA population model—do we need a new one.
32. S. R. HALL, D. G. MACMARTIN and D. S. BERNSTEIN 1993 *IEEE Transactions on Automatic Control* **38**, 1858–1862. Covariance averaging in the analysis of uncertain systems.
33. Y. KISHIMOTO and D. S. BERNSTEIN 1994 *Journal of Sound and Vibration* **182**, 59–76. Thermodynamic modelling of interconnected systems: II. dissipative coupling.
34. E. SKUDRZYK 1968 *Simple and Complex Vibratory Systems*. University Park: Pennsylvania State University Press.
35. D. G. MACMARTIN and S. R. HALL 1991 *Journal of Guidance, Control and Dynamics* **14**, 521–530. Control of uncertain structures using an H_∞ power flow approach.
36. A. BERMAN and R. J. PLEMMONS 1979 *Nonnegative Matrices in the Mathematical Sciences*. New York: Academic Press.
37. D. S. BERNSTEIN and D. C. HYLAND 1993. *SIAM Journal on Matrix Analysis and Applications* **14**, 880–901. Compartmental modeling and second-moment analysis of state space systems.
38. S. H. CRANDALL and W. D. MARK 1963 *Random Vibration in Mechanical Systems*. New York: Academic Press.
39. E. I. JURY 1965 *IEEE Transactions on Automatic Control*, **AC-10**, 110–111. A general formulation of the total square integrals for continuous systems.

APPENDIX A: NOTATION

S_{xx}	power spectral density matrix of x
S_{xy}	cross-spectral density matrix of x and y
j	$\sqrt{-1}$
I	identity matrix

e_i	i th column of I
\mathbf{e}	$[11 \cdots 1]^T$ (bold-face distinguishes from exponential)
$a_{(i)}$	i th element of column vector a
$A_{(k,l)}$	(k,l) -element of A
A_{ijkl}	$A_{(n_{ij}, n_{kl})}$
$A_{[ijk\ell]}$	(n_{ij}, n_{kl}) th 2×2 subblock of A
$\text{Re}[A], \text{Im}[A]$	real, imaginary part of A
$\text{diag}(a_1, \dots, a_r)$	diagonal matrix whose i th diagonal element is a_i
$\text{block-diag}(A_1, \dots, A_r)$	block-diagonal matrix whose i th diagonal block is A_i
A^T, A^*	transpose, complex conjugate transpose of A
$\text{tr}[A]$	trace of A
$\{A\}, \langle A \rangle$	diagonal, off-diagonal portion of A
$\text{Inc}[S], \text{Coh}[S]$	diagonal (incoherent), off-diagonal (coherent) portion of the spectral density (intensity) matrix S
$A > (\geq) 0$	symmetric positive (nonnegative) definite matrix

APPENDIX B: PROOF OF LEMMA 5.1

By substituting $\tilde{Q}_m = \tilde{Q}_{\text{Coh}} + \tilde{Q}_{\text{Inc}}$ and $D_m D_m^T = S_{w_m w_m} = \text{Coh}[S_{w_m w_m}] + \text{Inc}[S_{w_m w_m}]$ into equations (45)–(47), we obtain

$$P_{ij}^c = -(C_{m2} \tilde{Q}_{\text{Inc}} C_{m1}^T)_{ijj} - (C_{m2} \tilde{Q}_{\text{Coh}} C_{m1}^T)_{ijj}, \quad (181)$$

$$P_{ij}^d = -(C_{md} C_{m1} \tilde{Q}_{\text{Inc}} C_{m1}^T)_{ijj} - (C_{md} C_{m1} \tilde{Q}_{\text{Coh}} C_{m1}^T)_{ijj}, \quad (182)$$

$$P_{ij}^e = \frac{1}{2} (\text{Inc}[S_{w_m w_m}] B_m^T C_{m1}^T)_{ijj}. \quad (183)$$

Thus, from equation (51) it follows that

$$\hat{P}_{\text{Coh},ij} = (C_{m2} \tilde{Q}_{\text{Coh}} C_{m1}^T)_{ijj} = -(C_{md} C_{m1} \tilde{Q}_{\text{Coh}} C_{m1}^T)_{ijj},$$

which proves equations (98) and (99).

APPENDIX C: PROOF OF THEOREM 5.3

By summing equations (103) and (104) in Theorem 5.2 over the modes of each structure, it follows that

$$\mathcal{P}_i^c = \sum_{j=1}^{n_i} \sum_{k=1}^{n_i} \sigma_{ijk} (E_{ik}^{\text{th}} - E_{ij}^{\text{th}}) + \sum_{\substack{p=1 \\ p \neq i}}^r \sum_{j=1}^{n_i} \sum_{q=1}^{n_p} \sigma_{ijpq} (E_{pq}^{\text{th}} - E_{ij}^{\text{th}}) - \hat{\mathcal{P}}_{\text{Coh},i}, \quad (184)$$

$$\mathcal{P}_i^d = \sum_{j=1}^{n_i} \sigma_{ij} E_{ij}^{\text{th}} + \hat{P}_{\text{Coh},i}. \quad (185)$$

Since $\sigma_{ijk} = \sigma_{ikj}$ it follows that $\sum_{j=1}^{n_i} \sum_{k=1}^{n_i} \sigma_{ijk} (E_{ik}^{\text{th}} - E_{ij}^{\text{th}}) = 0$, while by substituting the definition of the modal thermodynamic energy (33) into the second term on the right-hand side of equation (184), we obtain

$$\sum_{\substack{p=1 \\ p \neq i}}^r \sum_{j=1}^{n_i} \sum_{q=1}^{n_p} \sigma_{ijpq} (E_{pq}^{\text{th}} - E_{ij}^{\text{th}}) = \sum_{\substack{p=1 \\ p \neq i}}^r \left(\sum_{q=1}^{n_p} \sum_{j=1}^{n_i} \sigma_{ijpq} \phi_{pq} \mathcal{E}_p^{\text{th}} - \sum_{j=1}^{n_i} \sum_{q=1}^{n_p} \sigma_{ijpq} \phi_{ij} \mathcal{E}_i^{\text{th}} \right)$$

$$\begin{aligned}
 &= \sum_{\substack{p=1 \\ p \neq i}}^r (\eta_{ip} \mathcal{E}_p^{\text{th}} - \eta_{pi} \mathcal{E}_i^{\text{th}}) \\
 &= \sum_{p=1}^r (\eta_{ip} \mathcal{E}_p^{\text{th}} - \eta_{pi} \mathcal{E}_i^{\text{th}}),
 \end{aligned}$$

which proves equation (109). Equation (110) follows from equation (185) in the same manner.

APPENDIX D: PROOF OF COROLLARY 6.1

By substituting $\tilde{A}_m = \bar{A}^{ipq} - \hat{A}^{ipq}$ into equation (107), we obtain

$$0 = \bar{A}^{ipq} \tilde{Q}_{pq} + \tilde{Q}_{pq} \bar{A}^{ipqT} - V^{ipq} + B_m e_{n_{pq}} e_{n_{pq}}^T B_m^T. \quad (186)$$

In equation (186), V^{ipq} includes the effect of coupling among all modes except the j th mode of the i th structure and the q th mode of the p th structure. To obtain the pairwise coupling coefficient $\bar{\sigma}_{ipq}$, we consider the Lyapunov equation without V^{ipq} , that is,

$$0 = \bar{A}^{ipq} \bar{Q}^{ipq} + \bar{Q}^{ipq} \bar{A}^{ipqT} + B_m e_{n_{pq}} e_{n_{pq}}^T B_m^T, \quad (187)$$

and from equation (105) of Theorem 5.2, the coupling coefficient $\bar{\sigma}_{ipq}$ given by

$$\bar{\sigma}_{ipq} = 2c_{ij} c_{pq} (C_{m1} \bar{Q}^{ipq} C_{m1}^T)_{ijj} = 2c_{ij} c_{pq} (\bar{Q}_{[ijj]}^{ipq})_{(2,2)}. \quad (188)$$

From equation (187), we obtain the matrix equations

$$0 = (A_{m[iij]} - \mathcal{A}_{[ijj]}) \bar{Q}_{[ijj]}^{ipq} + \bar{Q}_{[ijj]}^{ipq} (A_{m[iij]} - \mathcal{A}_{[ijj]})^T - \mathcal{A}_{[ijp]} \bar{Q}_{[ijp]}^{ipq} - \bar{Q}_{[pqj]}^{ipq} \mathcal{A}_{[ijp]}^T, \quad (189)$$

$$0 = (A_{m[iij]} - \mathcal{A}_{[ijj]}) \bar{Q}_{[ijp]}^{ipq} + \bar{Q}_{[ijp]}^{ipq} (A_{m[ipq]} - \mathcal{A}_{[pqj]})^T - \mathcal{A}_{[ijp]} \bar{Q}_{[pqj]}^{ipq} - \bar{Q}_{[ijj]}^{ipq} \mathcal{A}_{[pqj]}^T, \quad (190)$$

$$\begin{aligned}
 V &= (A_{m[ipq]} - \mathcal{A}_{[pqj]}) \bar{Q}_{[pqj]}^{ipq} + \bar{Q}_{[pqj]}^{ipq} (A_{m[ipq]} - \mathcal{A}_{[pqj]})^T \\
 &\quad - \mathcal{A}_{[pqj]} \bar{Q}_{[pqj]}^{ipq} - \bar{Q}_{[ijp]}^{ipq} \mathcal{A}_{[pqj]}^T,
 \end{aligned} \quad (191)$$

where

$$V \triangleq \begin{bmatrix} 0 & 0 \\ 0 & 1 \end{bmatrix}. \quad (192)$$

By using $\bar{Q}_{[pqj]}^{ipq} = \bar{Q}_{[ijp]}^{ipqT}$, we can obtain $\bar{Q}_{[ijj]}^{ipq}$ from equations (189)–(191). By substituting the resulting $\bar{Q}_{[ijj]}^{ipq}$ into equation (188), $\bar{\sigma}_{ipq}$ defined by equation (125) can also be obtained. Additionally, equations (126) and (128) can be obtained by subtracting equation (187) from equation (186), while defining $\hat{Q}^{ipq} \triangleq \bar{Q}_{pq} - \bar{Q}^{ipq}$ yields equation (128).

APPENDIX E: PROOF OF THEOREM 7.1

By setting $K_m = 0$, it follows that $\tilde{A}_m = A_m$. Thus the Lyapunov equation (48) can be rewritten as

$$A_m Q_m + Q_m A_m^T + \tilde{D}_m \tilde{D}_m^T = 0, \quad (193)$$

and the n_j th 2×2 diagonal sub-block $Q_{m[ij]}$ of Q_m is given by

$$A_{m[ij]} Q_{m[ij]} + Q_{m[ij]} A_{m[ij]}^T + V_{ij} = 0, \quad (194)$$

where

$$V_{ij} \triangleq \begin{bmatrix} 0 & 0 \\ 0 & a_{ij}^2 \end{bmatrix}. \quad (195)$$

Solving equation (194) and using equation (33) yields

$$Q_{m|ij} = \begin{bmatrix} \frac{a_{ij}^2}{4\zeta_{ij}\omega_{ij}} & 0 \\ 0 & \frac{a_{ij}^2}{4\zeta_{ij}\omega_{ij}} \end{bmatrix} = \begin{bmatrix} E_{ij}^{\text{th}} & 0 \\ 0 & E_{ij}^{\text{th}} \end{bmatrix}. \quad (196)$$

Thus,

$$E_{ij}^{\text{th}} = \frac{1}{2}[Q_{m(2n_{ij}-1, 2n_{ij}-1)} + Q_{m(2n_{ij}, 2n_{ij})}]. \quad (197)$$

On the other hand, from equation (115), E_{ij}^{bl} in equation (137) is given by

$$E_{ij}^{\text{bl}} = \frac{1}{2} \begin{bmatrix} \frac{\omega_{\xi, ij}^2}{\omega_{ij}^2} \tilde{Q}_{m(2n_{ij}-1, 2n_{ij}-1)} + \tilde{Q}_{m(2n_{ij}, 2n_{ij})} \end{bmatrix}. \quad (198)$$

Subtracting equation (198) from equation (197) yields

$$\hat{E}_{ij} = \frac{1}{2} \begin{bmatrix} (Q_m - \tilde{Q}_m)_{(2n_{ij}-1, 2n_{ij}-1)} + (Q_m - \tilde{Q}_m)_{(2n_{ij}, 2n_{ij})} & b_{ij}^2 \sum_{p=1}^r K_{ip} \\ & - \frac{\omega_{ij}^2}{\omega_{ij}^2} \tilde{Q}_{m(2n_{ij}, 2n_{ij})} \end{bmatrix}, \quad (199)$$

while subtracting equation (48) from equation (193) and setting $\hat{Q} = Q_m - \tilde{Q}_m$ yields equation (140). Finally, by substituting \hat{Q} into equation (199) we obtain equation (139).

APPENDIX F: PROOF OF PROPOSITION 9.1

Using equation (162), it follows that

$$\begin{aligned} (Z_m(j\omega) + L_m(j\omega))^{-1} &= (Z(j\omega) + \langle L_m(j\omega) \rangle)^{-1} \\ &= [Z(j\omega)(I + Z^{-1}(j\omega)\langle L_m(j\omega) \rangle)]^{-1} \\ &= (I + Z^{-1}(j\omega)\langle L_m(j\omega) \rangle)^{-1} Z^{-1}(j\omega) \\ &= (I - Z^{-1}(j\omega)\langle L_m(j\omega) \rangle) Z^{-1}(j\omega) + \mathcal{O}(\omega), \end{aligned}$$

which, with equations (15), (18) and (25), yields

$$(Z_m(j\omega) + L_m(j\omega))_{ijpq}^{-1} = \frac{(1/j\omega)\kappa_{ijpq}}{\hat{z}_{ij}(j\omega)\hat{z}_{pq}(j\omega)} + \mathcal{O}(\omega)_{ijpq}. \quad (200)$$

Using the integral formulas given in references [37,38], it follows that

$$\begin{aligned} \sigma_{ijpq} &= \int_{-\infty}^{\infty} \delta_{ijpq}(\omega) d\omega \\ &= \frac{1}{\pi} c_{ij} c_{pq} \int_{-\infty}^{\infty} \|[Z_m(j\omega) + L_m(j\omega)]_{ijpq}^{-1}\|^2 d\omega \end{aligned}$$

$$\begin{aligned}
 &= \frac{c_{ij}c_{pq}}{\pi} \int_{-\infty}^{\infty} \left| \frac{(1/j\omega)\kappa_{ijpq}}{\hat{z}_{ij}(j\omega)\hat{z}_{pq}(j\omega)} \right|^2 d\omega + \frac{c_{ij}c_{pq}}{\pi} \int_{-\infty}^{\infty} \delta_{ijpq}(j\omega) d\omega \\
 &= \frac{\kappa_{ijpq}^2(c_{ij} + c_{pq})}{(\hat{\omega}_{ij}^2 - \hat{\omega}_{pq}^2)^2 + (c_{ij} + c_{pq})(c_{ij}\hat{\omega}_{pq}^2 + c_{pq}\hat{\omega}_{ij}^2)} + \frac{c_{ij}c_{pq}}{\pi} \int_{-\infty}^{\infty} \delta_{ijpq}(j\omega) d\omega,
 \end{aligned}$$

which proves equation (164).

APPENDIX G: PROOF OF PROPOSITION 10.1

For $i=1, \dots, r$ and $j=1, \dots, n_i$, let $\Delta\omega_{ij}$ denote disjoint frequency bands such that

$$\lim_{\zeta_{ij} \rightarrow 0} \int_{\Delta\omega_{ij}} \frac{1}{z_{ij}(j\omega)} d\omega = \int_{-\infty}^{\infty} \frac{1}{z_{ij}(j\omega)} d\omega. \quad (201)$$

Furthermore, since $K_{\{im\}} \rightarrow 0$ implies that $L(j\omega) + Z_s(j\omega) \rightarrow Z_s(j\omega)$ and $L_m(j\omega) + Z_m(j\omega) \rightarrow Z_m(j\omega)$, it follows from equations (31), (63), and (93) that

$$\begin{aligned}
 \lim_{\substack{K_{\{im\}} \rightarrow 0 \\ \zeta_{\{ij\}} \rightarrow 0}} \hat{P}_i &= \lim_{\substack{K_{\{im\}} \rightarrow 0 \\ \zeta_{\{ij\}} \rightarrow 0}} \frac{1}{2\pi} \int_{-\infty}^{\infty} (T_i(j\omega)T_i^*(j\omega)[L(j\omega) + Z_s(j\omega)]_{(i,\delta)}^{-*} \\
 &\quad - \sum_{j=1}^{n_i} [D_m D_m^T (L_m(j\omega) + Z_m(j\omega))^{-*}]_{ijij}) d\omega \\
 &= \lim_{\zeta_{\{ij\}} \rightarrow 0} \frac{1}{2\pi} \int_{-\infty}^{\infty} (T_i(j\omega)T_i^*(j\omega)z_i(j\omega)^{-*} - \sum_{j=1}^{n_i} [D_m D_m^T Z_m(j\omega)^{-*}]_{ijij}) d\omega \\
 &= \lim_{\zeta_{\{ij\}} \rightarrow 0} \frac{1}{2\pi} \int_{-\infty}^{\infty} \left[z_i(j\omega) \sum_{j=1}^{n_i} \frac{a_{ij}b_{ij}}{z_{ij}(j\omega)} z_i^*(j\omega) \sum_{j=1}^{n_i} \frac{a_{ij}b_{ij}}{z_{ij}^*(j\omega)} z_i^{-*}(j\omega) - \sum_{j=1}^{n_i} \frac{a_{ij}^2}{z_{ij}^*(j\omega)} \right] d\omega \\
 &= \lim_{\zeta_{\{ij\}} \rightarrow 0} \frac{1}{2\pi} \int_{-\infty}^{\infty} \left[\left(\sum_{j=1}^{n_i} \frac{b_{ij}^2}{z_{ij}(j\omega)} \right)^{-1} \sum_{j=1}^{n_i} \frac{a_{ij}b_{ij}}{z_{ij}(j\omega)} \sum_{j=1}^{n_i} \frac{a_{ij}b_{ij}}{z_{ij}^*(j\omega)} - \sum_{j=1}^{n_i} \frac{a_{ij}^2}{z_{ij}^*(j\omega)} \right] d\omega \\
 &= \frac{1}{2\pi} \sum_{j=1}^{n_i} \int_{\Delta\omega_{ij}} \left[\left(\sum_{j=1}^{n_i} \frac{b_{ij}^2}{z_{ij}(j\omega)} \right)^{-1} \sum_{j=1}^{n_i} \frac{a_{ij}b_{ij}}{z_{ij}(j\omega)} \sum_{j=1}^{n_i} \frac{a_{ij}b_{ij}}{z_{ij}^*(j\omega)} - \sum_{j=1}^{n_i} \frac{a_{ij}^2}{z_{ij}^*(j\omega)} \right] d\omega \\
 &= \frac{1}{2\pi} \sum_{j=1}^{n_i} \int_{\Delta\omega_{ij}} \left[\frac{a_{ij}^2}{z_{ij}^*(j\omega)} - \frac{a_{ij}^2}{z_{ij}^*(j\omega)} \right] d\omega \\
 &= 0.
 \end{aligned}$$

APPENDIX H: PROOF OF PROPOSITION 10.2

As $K_{\{im\}} \rightarrow 0$, it follows that $\tilde{Q}_m \rightarrow Q_m$, where the diagonal elements of Q_m are given by equation (196). Furthermore, since disturbances entering different structures are mutually uncorrelated, it follows that modal coherence does not occur between modes of different structures. Hence the 2×2 (n_{ip}, n_{iq}) off-diagonal sub-block of Q_m satisfies

$$A_{m[ip]} Q_{m[ipiq]} + Q_{m[iq]} A_{m[iq]}^T + V_{ipq} = 0, \quad i = 1, \dots, r, \quad p, q = 1, \dots, n_i, \quad (202)$$

where

$$V_{ipq} \triangleq \begin{bmatrix} 0 & 0 \\ 0 & a_{ip} a_{iq} \end{bmatrix}. \quad (203)$$

Solving equation (202) in closed form yields

$$Q_{m[ipiq]} \triangleq \begin{bmatrix} \frac{2\omega_{ip}\omega_{iq}(\omega_{ip} + \omega_{iq})a_{ip}a_{iq}\zeta_{ij}}{D} & \frac{\omega_{ip}(\omega_q^2 - \omega_{ip}^2)a_{ip}a_{iq}}{D} \\ \frac{\omega_{iq}(\omega_{ip}^2 - \omega_{iq}^2)a_{ip}a_{iq}}{D} & \frac{2\omega_{ip}\omega_{iq}(\omega_{ip} + \omega_{iq})a_{ip}a_{iq}\zeta_{ij}}{D} \end{bmatrix}, \quad (204)$$

where

$$D \triangleq (\omega_{ip}^2 - \omega_{iq}^2)^2 + 32\omega_{ip}^2\omega_{iq}^2\zeta_{ij}^2 + 16\omega_{ip}\omega_{iq}\zeta_{ij}^2(\omega_{ip}^2 + \omega_{iq}^2).$$

Furthermore, it can be shown that

$$(E_0^{-1/2} Q_m E_0^{-1/2})_{[ipiq]} = E_{0[ipip]}^{-1/2} Q_{m[ipiq]} E_{0[iqiq]}^{1/2}. \quad (205)$$

By substituting $Q_{m[ipiq]}$ given by equation (204) into equation (205) and letting $\zeta_{\{ij\}} \rightarrow 0$, we obtain

$$\lim_{\substack{K_{\{im\}} \rightarrow 0 \\ \zeta_{\{ij\}} \rightarrow 0}} (E_0^{-1/2} \tilde{Q}_m E_0)^{-1/2}_{[ipiq]} = \lim_{\zeta_{\{ij\}} \rightarrow 0} (E_0^{-1/2} Q_m E_0^{-1/2})_{[ipiq]} = I. \quad (206)$$

Thus, equation (172) follows immediately from equations (196) and (206).

APPENDIX I: PROOF OF PROPOSITION 10.3

By using \tilde{Q}_{Inc} given by equation (101) in Lemma 5.1, we obtain

$$\lim_{K_{\{m\}} \rightarrow 0} P_{ij}^d = \lim_{K_{\{m\}} \rightarrow 0} [-(C_{\text{md}} C_{\text{m1}} \tilde{Q}_{\text{Inc}} C_{\text{m1}}^T)_{ijj} + \hat{P}_{\text{Coh},ij}]. \quad (207)$$

Next, by using equation (101), note that $K_{\{im\}} \rightarrow 0$ implies that $\tilde{Q}_{\text{Inc}} \rightarrow \tilde{Q}_{\text{Inc},0}$, which satisfies

$$0 = A_m \tilde{Q}_{\text{Inc},0} + \tilde{Q}_{\text{Inc},0} A_m^T + \text{Inc}[S_{w_m w_m}]. \quad (208)$$

By using the energy co-ordinates defined by equation (115) it follows that

$$-\lim_{K_{\{m\}} \rightarrow 0} (C_{\text{md}} C_{\text{m1}} \tilde{Q}_{\text{Inc}} C_{\text{m1}}^T)_{ijj} = -(C_{\text{md}} C_{\text{m1}} \tilde{Q}_{\text{Inc},0} C_{\text{m1}}^T)_{ijj} = -a_{ij}^2/2. \quad (209)$$

Therefore,

$$\lim_{K_{i(m)} \rightarrow 0} P_{ij}^d = -a_{ij}^2/2 + \lim_{K_{i(m)} \rightarrow 0} \hat{P}_{\text{Coh},ij}. \quad (210)$$

On the other hand, by calculating P_{ij}^e directly from equation (183) yields

$$\lim_{K_{i(m)} \rightarrow 0} P_{ij}^e = a_{ij}^2/2. \quad (211)$$

By using equations (210), (211), $\lim_{K_{i(m)} \rightarrow 0} P_{ij}^c = 0$, and equation (51), we obtain

$$0 = \lim_{K_{i(m)} \rightarrow 0} (P_{ij}^d + P_{ij}^e) = -a_{ij}^2/2 + \lim_{K_{i(m)} \rightarrow 0} \hat{P}_{\text{Coh},ij} + a_{ij}^2/2 = \lim_{K_{i(m)} \rightarrow 0} \hat{P}_{\text{Coh},ij}. \quad (212)$$

It now follows from equation (111) that $\lim_{K_{i(m)} \rightarrow 0} \hat{\mathcal{P}}_{\text{Coh},i} = \lim_{K_{i(m)} \rightarrow 0} \sum_{j=1}^{n_i} \hat{P}_{\text{Coh},ij} = 0$.